Use of Triply Periodic Minimal Surface Lattices for Heat Transfer Applications: A Systematic Literature Investigation

energies

MDPI

Systematic Review

Use of Triply Periodic Minimal Surface Lattices for Heat Transfer Applications: A Systematic Literature Investigation

Laura Savoldi [1,*], Antonio Cammi [2,3], William Ferretto [2], Alessio Quamori Tanzi [1] and Luca Marocco [2]

[1] MAHTEP Group, Dipartimento Energia "Galileo Ferraris", Politecnico di Torino, Corso Duca degli Abruzzi 24, 10129 Torino, Italy; alessio.quamori@polito.it
[2] Department of Energy, Politecnico di Milano, Via Lambruschini 4, 20156 Milano, Italy; antonio.cammi@polimi.it (A.C.); william.ferretto@polimi.it (W.F.); luca.marocco@polimi.it (L.M.)
[3] Department of Mechanical and Nuclear Engineering, Khalifa University of Science and Technology, Abu Dhabi 127788, United Arab Emirates
* Correspondence: laura.savoldi@polito.it

Abstract

The scientific interest in Triply Periodic Minimal Surface (TPMS) lattices for thermal applications has grown exponentially in recent years, largely driven by the advances in additive manufacturing. However, the lack of a transparent and reproducible selection methodology in previously published reviews hinders the clarity and comparability of findings. This paper adopts and customizes the APISSER framework, a structured and repeatable method that guides literature reviews through five steps: defining research questions, identifying sources, screening studies, extracting data, and reporting results. This approach is applied to investigate the use of TPMS lattices in heat-transfer applications, including heat sinks and heat exchangers. The study covers 170 peer-reviewed journal articles from 2000 to 2024, analyzing key aspects such as application domain, topology, working fluid, flow regime, additive manufacturing method, and numerical modeling details. Results show a predominance of numerical studies, with the Gyroid and Diamond topologies being the most investigated. These structures are frequently modeled as porous media, especially for estimating pressure drops, although detailed thermal analysis often relies on full-resolution geometries. Water and air are the most common working fluids, while turbulence modeling remains limited to RANS approaches. The structured methodology adopted ensures high reproducibility and provides a quantitative foundation for addressing the identified knowledge gaps, guiding future experimental and computational research.

Keywords: Triply Periodic Minimal Surface lattices; heat transfer; APISSER; heat sinks; heat exchangers

Academic Editor: Rafik Belarbi

Received: 2 December 2025
Revised: 14 January 2026
Accepted: 2 February 2026
Published: 4 February 2026

1. Introduction

In the field of advanced heat-transfer applications, Triply Periodic Minimal Surfaces (TPMSs) have emerged as a promising solution. TPMS are periodic surfaces characterized by zero mean curvature and no self-intersections, typically defined through trigonometric (sine and cosine) functions in the three spatial directions. Their distinctive advantage lies in their highly interconnected and complex lattice architecture, which increases the surface area-to-volume ratio and promotes efficient heat exchange. At the same time, the smooth and continuous nature of TPMS, free of sharp edges and dead zones, helps minimize pressure losses, enabling enhanced convective heat transfer with low flow resistance.

Among their various uses, TPMS have shown particular potential in heat sinks (HS) and heat exchangers (HX).

Despite being relatively recent in the context of heat transfer research, several review papers have already been published on TPMS applications [1–4]. These reviews address topics such as TPMS design, recent advancements, application potential in HS and HX, and fabrication via additive manufacturing (AM) techniques.

In Dutkowski et al. [1], approximately 120 publications are analyzed, including studies focusing on the mechanical and manufacturing aspects of TPMS lattices. The authors emphasize the limited availability of experimental data on thermal performance and advocate broader CFD-based exploration of TPMS topologies beyond the most frequently studied ones. They also highlight the need for an interdisciplinary approach to support the development of TPMS-based thermal systems.

Yeranee and Rao [2] provide a focused review on heat-transfer applications of TPMS lattices, particularly in HS and HX, considering topologies such as Gyroid, Diamond, Primitive, and I-WP. Around 100 studies are analyzed, primarily numerical, covering both laminar and turbulent regimes, and exploring the influence of design parameters, such as porosity, wall thickness, and unit cell size, on thermal and fluid-dynamic performance. The review also includes an overview of AM techniques suitable for TPMS fabrication. Given the increasing feasibility of producing and testing TPMS in experimental setups, the authors stress the importance of experimental validation. They suggest techniques such as liquid crystal thermography, thermocouples, and MRI for characterizing flow and temperature fields. A key limitation identified is the lack of reliable heat-transfer correlations at high Reynolds numbers, underscoring the need for further experimental campaigns and optimization studies.

The review published in 2024 by Gado et al. [3] includes a bibliometric keyword analysis of around 150 papers. It extends the scope of covered topologies (including Neovius, FKS, and FRD) and reviews both HS and HX applications, with air and water as the most common working fluids. The paper summarizes computational studies, details friction factor and Nusselt correlations, and provides insights into numerical software and AM methods. It also outlines emerging applications of TPMS-based components, including compact heat exchangers, latent heat thermal energy storage (TES), adsorption systems, battery thermal management, and membrane distillation. Additional use cases are identified in photovoltaic (PV) and fuel cell thermal control, desalination systems, atmospheric water harvesting, carbon capture, thermochemical sorption energy storage, and desiccant-based air conditioning. However, the bibliometric analysis has been used only to identify relevant papers, and the review does not provide a systematic categorization of the literature based on criteria or attributes that would help readers quickly locate studies on specific topics (e.g., Diamond-topology heat sinks using water as the working fluid under turbulent conditions).

This specific point is partly addressed by the most recent review by Wang et al. [4], published in 2025, which focuses exclusively on the flow and heat-transfer performance of TPMS. It analyzes more than 90 papers dealing with the applications of TPMS to thermal management systems, among which are HS and HX. The effect of unit cell size is addressed, and several topologies are analyzed, with a comparison to traditional designs. Notwithstanding the valuable information provided by [4], it partially fails to facilitate navigation in the paper database, as it emphasizes comparing results across scholars rather than the features that characterize the analyses.

Despite the valuable insights provided by these reviews, a significant limitation common to all is the lack of clarity, transparency, and reproducibility in the methodology used to select the reviewed publications. Even in [3] and [4], the inclusion criteria are not

explicitly defined, making it difficult to assess the completeness and potential biases of the findings. A standardized, transparent, and reproducible paper selection process would enhance the reliability and scope of future reviews. As also highlighted in [3] and [4], the TPMS research domain is evolving rapidly, underscoring the need for regular updates to track emerging trends and innovations. However, systematic reviews can be conducted effectively only if supported by a clear, rigorous methodology for identifying and classifying the relevant literature.

The objective of this paper is to conduct, for the first time, a comprehensive and systematic literature investigation of TPMS applications in heat transfer problems, based on a structured selection and analysis framework. The adopted methodology is the APISSER framework [5], a task-oriented extension of the PRISMA protocol [6], specifically tailored to engineering-focused reviews that require metadata classification and topic filtering.

This investigation includes peer-reviewed journal articles published in English between 2000 and 2024, identified through a keyword-based search combined with explicit inclusion and exclusion criteria. For each paper, a consistent set of attributes, such as the experimental or numerical nature of the study, the modeling and geometry-generation tools employed, the working fluids, the flow regime, the AM technique, and the presence of validation, is extracted, allowing the construction of a structured database.

This categorization goes beyond the scope of previous reviews (e.g., [4]), which typically focused on comparing thermal figures of merit. Here, the metadata-driven approach provides a broader, systematic perspective on publication trends, modeling practices, and geometric choices, thereby enabling a more comprehensive mapping of the state of the art. The method adopted for the analysis allows, as a byproduct, the sorting of papers based on a specific attribute among those used to categorize them. The paper list, reported in the reference section in alphabetic order to ease the identification of the scholar contributions, and the corresponding database, available in the Supplementary Materials, can become a viable tool for finding research works that better address a specific aspect of interest (e.g., papers dealing with heat sinks, with experimental investigations involving air under laminar flow conditions). This transparent and repeatable approach improves the robustness of the findings and allows researchers to contextualize their work within the broader scientific landscape and identify gaps and underexplored areas. Unlike other reviews, the novelty of the present work lies in the metadata-driven structure enabled by the APISSER methodology, rather than in the number of papers reviewed. By systematically extracting and cross-correlating a consistent set of attributes, this approach allows the identification of relationships between TPMS topology, application domain, flow regime, modeling strategy, and validation practices that were not accessible in previous reviews. In particular, the APISSER framework makes it possible to highlight systematic biases in modeling choices, recurring gaps in experimental validation, and inconsistencies in performance evaluation metrics, thereby providing a framework to contextualize and interpret current conclusions in the literature.

The structure of the paper is as follows: Section 2 presents the APISSER framework and its application to this review. Section 3 discusses the main results of the analysis, while Section 4 provides a focused application of the method to studies involving Gyroid and Diamond TPMS used in HS and HX. Final remarks and conclusions are given in Section 5.

2. Methodology

This section outlines the selected methodology for conducting a systematic literature investigation adaptable for various engineering applications. The APISSER framework was adopted to structure data extraction and classification, while PRISMA 2020 guidelines were followed to ensure transparent reporting of the review process. APISSER is an acronym

that stands for "A-priori, Paper identification, Inclusion/Exclusion screening, Selection, Structured data extraction, Evaluation, and Reporting". It consists of the five phases shown in Figure 1, to be rigorously followed in the given order to ensure reproducibility.

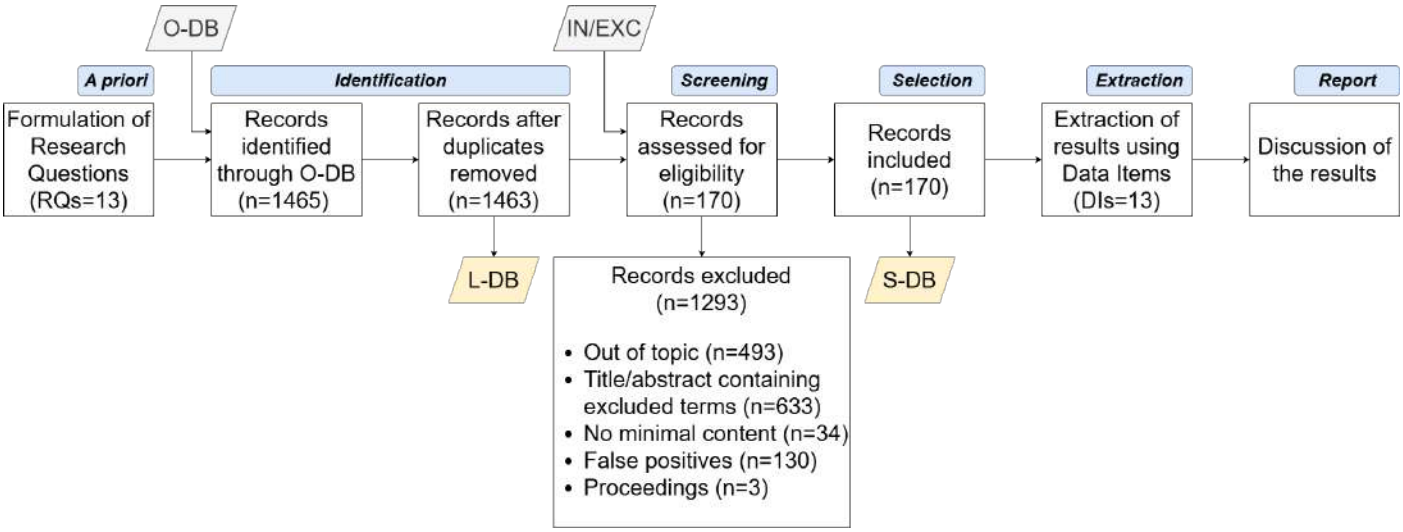

Figure 1. Flow chart of the APISSER methodology, together with the results of the identification and screening process used to construct the S-DB. The acronyms are explained in the text.

The process begins with the "A-priori phase", which establishes the foundation for the literature review. In this phase, specific knowledge gaps or problems within the topic of interest are identified and addressed through the formulation of precise "Research Questions" (RQs). The RQs are specific and focused on covering the areas where knowledge is lacking or fragmented; the more RQs are formulated, the more comprehensive the literature analysis will be. Collectively, the RQs should ensure the full coverage of the overall knowledge gap. The answers to the RQs automatically result in a set of attributes, based on which the papers in the database can be easily categorized and sorted.

The "Identify phase" involves the creation of a database of potentially relevant papers. This phase begins with the selection of appropriate "Online Databases" (O-DB), such as Scopus [7], Web of Science [8], or IEEE Xplore [9], depending on the field of study. The outcome of this phase is the so-called "Long Database" (L-DB), populated with publications that could potentially address the RQs. A detailed keyword query strategy is designed to retrieve potential papers by combining technical terms with related application areas. Boolean operators are utilized to refine the search criteria based on the specific O-DB. To assess whether the selected keywords are appropriate, the L-DB is compared against a set of benchmark publications known to be relevant in the field.

The "Screen & Select phase" refines the L-DB into a more focused Short Database (S-DB) by applying explicit eligibility criteria to systematically include or exclude papers. The process is conducted in two stages: an initial rapid assessment of titles and abstracts, followed by a detailed evaluation of the full texts for the studies that pass the preliminary check. To ensure reproducibility, each step of the selection procedure is documented in detail, allowing other researchers to replicate the methodology and achieve comparable results. Inclusion criteria (IN) define the essential requirements for selection, such as publication date, language, peer-review status, relevance to the topic, and alignment with the intended use case. In addition, a specific exclusion criterion (EXC1) is introduced to remove studies whose primary focus lies outside TPMS thermal applications, for example, works dealing mainly with mechanical properties, scaffolds, bone tissue, or fatigue. Papers that do not satisfy all the inclusion criteria, or that fall within EXC1, are not retained in the final dataset.

The "Extract phase" is devoted to the extraction of "Data Items" (DIs), each explicitly linked to one or more RQs. The DIs are the main content of the investigation and serve as the basis for the subsequent Report phase. The number and type of DI extracted are, to some extent, subjective, as they may vary depending on the objectives and topics of the investigation. Some DIs may be subcategories or combinations of others, which allows more focused findings; for example, an author might choose to investigate experimental papers specifically authored by European researchers, combining geographic and methodological aspects to refine the literature investigation.

Finally, the "Report phase" synthesizes the extracted data and communicates the findings in a structured format. The results are summarized to directly address the RQs. The results are categorized to capture trends that emerged from the analysis. This also provides relevant insights for identifying research gaps to address in the future.

The completed PRISMA 2020 checklist and flow diagram have been provided as Supplementary Materials.

2.1. A Priori Phase

The topic of this systematic investigation is the application of TPMS in heat transfer problems, according to the 13 RQs synthetically reported in Table 1 and briefly commented on in the following section.

Table 1. Research questions addressed in the systematic investigation.

ID	Research Question
RQ1	Which countries have contributed most to TPMS research?
RQ2	In which years has TPMS research grown the most?
RQ3	Which are the most common scopes for the use of TPMS in thermal applications?
RQ4	Which are the specific applications of TPMS in heat transfer problems?
RQ5	Do studies rely on experiments, simulations, or both?
RQ6	Which tools are commonly used to generate TPMS geometries for thermal applications?
RQ7	Which are the most used working fluids in TPMS heat transfer studies?
RQ8	Which AM methods are most commonly adopted?
RQ9	Which CFD software is most used in thermal TPMS studies?
RQ10	Which TPMS topologies are most frequently investigated in thermal applications?
RQ11	Which flow regimes are typically studied in TPMS structures for thermal applications?
RQ12	Which turbulence closure models are most frequently adopted?
RQ13	Do studies include any validations of the numerical results vs. experimental data?

With the growing activity in TPMS research in recent years, it may be relevant to identify the geographical distribution of publications (RQ1) to understand where scientific and technological research is most active in this field. At the same time, monitoring the growth in research volume over recent years (RQ2) and analyzing its rate could help understand if and how studies related to TPMS are still considered a relevant research direction. While RQ1 and RQ2 provide contextual information on the geographical and temporal evolution of TPMS research, the core scientific insights of the present investigation primarily rely on RQ3 to RQ13, which address scope and applications, modeling practices, topology–application relationships, flow regimes, turbulence closures, and validation strategies. These research questions form the backbone of the critical analysis presented in Sections 3 and 4.

TPMS offers a promising solution for improving heat transfer across a variety of applications, including pure heat transfer in HS and HX. Some investigations focus specifically on the hydrodynamic behavior within TPMS lattices. Although the hydraulic behavior is intrinsically related to heat transfer, it is not considered directly relevant to this

investigation, see also below. Beyond purely thermal scopes, some studies are more closely related to chemical processes, addressing phenomena such as mass transfer, absorption, or the behavior of phase-change materials (PCMs) within TPMS lattices. The diversity of these topics makes it relevant to identify the scope of each contribution (RQ3).

When narrowing the analysis to heat-transfer applications, it is necessary to specify the operational context in which each TPMS study is conducted (RQ4). Excluding purely bibliographic contributions, the literature can be grouped into the following main categories:

- Heat sinks (HS), where TPMS lattices are used to enhance thermal dissipation from solid surfaces through single-phase forced convection.
- Heat exchangers (HX), in which TPMS structures enable heat transfer between two separate fluid streams, often aiming to maximize compactness and surface area while limiting pressure drop.
- Free convection (FC) systems, where natural buoyancy effects govern fluid motion, typically in low-power or passive cooling scenarios involving air.
- Material-centered (TP, which stands for thermal properties) studies, which focus on the effective thermal conductivity or storage capacity of TPMS-based solids, including configurations with embedded PCMs.

Studies focusing on heat transfer in TPMS lattices use different methodological approaches: some rely solely on experimental work, others on numerical simulations, and a third group combines both. Experimental investigations are essential for validating results and for capturing complex physical behaviors that may not be fully represented in simulations. On the other hand, numerical studies, often based on CFD, offer the flexibility to explore a wider range of operating conditions, geometries, and parameters. Identifying the methodological approach used in each study is therefore crucial for assessing the robustness of the results and guiding future research (RQ5).

Generating TPMS structures requires specialized software that may vary in modeling flexibility, meshing efficiency, and compatibility with 3D printing or CFD environments. The variety of tools used for TPMS geometry generation, which has never been systematically investigated in previous reviews, is addressed in RQ6.

Different studies use various working fluids depending on the specific application. Common choices include air and water, while more specialized studies investigate other gases, molten salts, water–glycol mixtures, and PCMs such as paraffin (RQ7).

For studies reporting experimental investigations of TPMS, it is relevant to understand the manufacturing methodology used to 3D print the lattice (RQ8), as it may affect the measured results. Surface roughness may, for instance, affect pressure drop and heat transfer performance.

For the studies reporting numerical investigations, various software tools could be employed for numerical analysis, relying either on different approaches, e.g., Finite volume, Finite elements, Lattice Boltzmann, and others. It is therefore relevant to consider what numerical method and tool were adopted for the analysis (RQ9), an aspect that has not received much attention in previous reviews.

Among the various TPMS structures, each topology offers distinct advantages depending on the intended application. Gyroid and Diamond lattices are the most extensively investigated, owing to their favorable thermo-hydraulic behavior. They generally achieve higher heat-transfer rates than simpler geometries such as Primitive or Neovius, while inducing lower pressure drops than more intricate structures like Lidinoid or SplitP. Understanding how these topologies are distributed across different use cases is therefore essential for identifying emerging research directions and for contextualizing performance comparisons presented in previous narrative reviews, which typically emphasize figures of merit rather than providing a comprehensive mapping of topology usage (RQ10).

In addition to selecting the most suitable topology, the effectiveness of TPMS designs in heat-transfer applications also depends on the flow conditions, particularly whether the flow is laminar or turbulent. Investigating the most frequently studied flow regimes (RQ11) can provide valuable insights into TPMS behavior across different operating scenarios and highlight gaps in current research.

For numerical studies involving turbulent flows, the choice of turbulence closure model (RQ12) plays a key role. Identifying which models, such as Standard or Realizable k-ε,or k-ω SST, are most commonly adopted and can offer practical guidance for future simulations. This is particularly relevant when results are benchmarked against experimental data.

Finally, attention must be paid to the degree of validation provided for numerical findings (RQ13). While verification through mesh sensitivity analysis is often reported, actual validation—intended as a comparison with measured data—is less common. Understanding which studies include such comparisons, and under what conditions, helps assess the overall reliability of the current numerical literature on TPMS-based systems.

2.2. Identify Phase

The bibliographic search is conducted using the O-DB Scopus [7], selected for its comprehensive coverage of peer-reviewed literature in engineering and applied sciences. A dedicated query (Equation (1)) is designed using Boolean operators. These operators, such as `AND`, `OR`, and `AND NOT`, allow for flexible and controlled combinations of keywords, enabling a targeted refinement of the search results. For a detailed explanation of Boolean syntax in Scopus, the reader is referred to the official guidelines available at: https://service.elsevier.com/app/answers/detail/a_id/11365/supporthub/scopus/#tips (accessed on 16 October 2025).

$$
\begin{aligned}
&(\text{TITLE-ABS-KEY}((\text{tpms}) \text{ OR } (\text{“triply periodic” W/2 “minimal surfaces”}))\\
&\quad \text{AND KEY}\Big(\text{tpms OR “triply periodic minimal surfaces” OR thermal}\\
&\qquad \text{OR “energy efficiency” OR “experimental validation” OR modeling}\\
&\qquad \text{OR turbulence OR “turbulent flow” OR “laminar flow”}\\
&\qquad \text{OR “numerical simulation” OR gyroid OR diamond}\\
&\qquad \text{OR schwartz OR primitive OR splitP}\\
&\qquad \text{OR Neovius OR topology OR “additive manufacturing”}\\
&\qquad \text{OR design OR “3-d printing” OR “heat sink”}\\
&\qquad \text{OR “heat exchanger” OR “heat transfer” OR “porous media”}\\
&\qquad \text{OR “cellular material” OR lattices OR CFD}\Big)\\
&\quad \text{AND PUBYEAR} < 2025)\\
&\quad \text{AND LIMIT-TO}(\text{SRCTYPE}, \text{“j”})\\
&\quad \text{AND LIMIT-TO}(\text{PUBSTAGE}, \text{“final”})\\
&\quad \text{AND LIMIT-TO}(\text{DOCTYPE}, \text{“ar”})\\
&\quad \text{AND LIMIT-TO}(\text{LANGUAGE}, \text{“English”})
\end{aligned}
\tag{1}
$$

During the initial search, additional filters are applied directly within Scopus to narrow down the results and generate the L-DB. These filters correspond to inclusion criteria IN0 through IN3, which are summarized in Table 2. Note that automated database searches frequently miss relevant papers due to inconsistencies or omissions in keyword usage. For instance, the hooking of certain papers clearly discussing TPMS may be excluded be-

cause they use variations like "Triply periodic minimum (instead of minimal) surface" [10]. Furthermore, some papers refer to TPMS implicitly by referencing general terms such as "lattices" [11] without explicitly mentioning TPMS in their titles, keywords, or abstracts. Others specify particular TPMS types, such as Gyroid or Diamond, without directly mentioning the acronym TPMS itself. Although careful reading confirms that those papers (for instance [12,13]) actually focus on TPMS, they remain difficult to locate through automated query methods. This problem underscores the importance of consistently and explicitly including key terms, such as TPMS, in the title, abstract, or keywords to increase the paper's visibility and accessibility. The acronym TPMS, however, does not unambiguously identify Triply Periodic Minimal Surfaces, as it could also stand for Two-Phase ModelS, as in [14], or for "Thermal Protection MaterialS (TPMs)", or "Tire Pressure Monitoring System", "Translational Parallel ManipulatorS" etc, giving a number of false-positive items in the L-DB. These papers have obviously been ruled out from the S-DB in the "Screen-and-Select" phase.

Table 2. Inclusion and exclusion criteria for the selection of papers.

ID	Type	Requirement
IN0	Type of publication	Journal paper
IN1	Years considered	$2000 \leq \text{YEAR} \leq 2024$
IN2	Language	English
IN3	Peer-reviewed	Yes
IN4	Topic	Thermal-hydraulic studies involving TPMS
IN5	Minimal content requirement	Heat exchangers, heat sinks, or other thermal applications
IN6	Subject area	Engineering, Science and Technology, or Medicine
EXC1	Terms to exclude	mechanical properties, scaffold, bone, fatigue

2.3. Screen-and-Select Phase

This phase refines the L-DB to extract only those documents aligned with the specific objectives of this investigation. The screening begins by evaluating titles and abstracts for coherence with the topic, i.e., the use of TPMS for heat transfer applications. Papers unrelated to this focus are discarded.

During this step, exclusion criterion EXC1 is applied. This removes studies primarily concerned with mechanical performance or biological applications, such as those referring to "scaffold", "bone", or "fatigue." Importantly, EXC terms are not excluded from the initial Scopus query, since papers containing these terms may still offer useful insights for heat transfer applications, e.g., those addressing lattice permeability, provided they explicitly mention thermal aspects. Nevertheless, 633 studies were discarded for both having an excluded term in the title and being off-topic.

After title and abstract screening, a full-text review is carried out. Each paper was independently reviewed by at least two authors to reduce selection and extraction bias, with no automatic procedure for the selection. Only studies satisfying the remaining inclusion criteria—specifically those addressing "thermal-hydraulic TPMS applications" (IN4), those presenting "at least one thermal use case" (IN5), and those related to specific subject areas (IN6)—are retained. The inclusion criteria guaranteed the exclusion of 493 studies for being "out of topic" and 34 studies for "not providing minimal content". During this stage, false positives from the earlier query are filtered out. Moreover, several studies dealing only with hydraulic aspects (such as determination of the lattice permeability, see [15–29]), but with no link to thermal applications are identified and filtered out.

The resulting set of documents constitutes the S-DB, which includes only the core studies and is provided as Supplementary Materials.

2.4. Extract Phase

The "Extract phase" is devoted to the identification and registration of a set of Data Items, which were selected to comprehensively address the knowledge gaps outlined in the RQs reported in Table 1. In this context, each DI, reported in Table 3, serves as a container for information or attributes extracted from the selected studies, contributing directly to answering one or more RQs. Depending on the scope of the analysis, statistical observations can be derived either from individual DIs or from correlations among multiple items.

Table 3. Data Items selected for the evaluation of the results.

ID	Data Item
DI1	Country of the publication
DI2	Year of publication
DI3	Scope of the study
DI4	Specific application within the heat transfer domain
DI5	Focus of the study: experimental, numerical, or both
DI6	TPMS geometry generation tool
DI7	Working fluid used in the study
DI8	Additive manufacturing (AM) method
DI9	Numerical software employed
DI10	TPMS topology (e.g., Gyroid, Diamond, etc.)
DI11	Flow regime: laminar, turbulent, or transitional
DI12	Turbulence model (for turbulent simulations)
DI13	Presence of validation (experimental or numerical)

3. Results of the Investigation

This section presents the results of the systematic investigation conducted using the APISSER framework, corresponding to the final Report phase. From an initial pool of over 1400 papers collected in the L-DB, a total of 170 studies were selected and included in the S-DB [30–199], excluding the three review papers previously discussed. Each of the following subsections analyzes the selected studies with reference to one or more specific DIs, as defined in the methodology. In addition to reporting quantitative distributions, the following sections provide a critical interpretation of the observed trends, highlighting the underlying physical, methodological, and practical drivers shaping current TPMS research.

3.1. DI1 and DI2: Country and Year of the Publications

The map in Figure 2 illustrates the global distribution of scientific contributions on the topic of interest, based on the affiliation of the first author of the paper. Each country is colored according to the number of published studies, with darker shades indicating higher research activity. China leads the worldwide picture significantly with 77 publications, followed by the United Arab Emirates (21), Canada (11), the United States (9), Italy, Japan, and Poland (5). Countries without contributions are colored with the lightest colour. This visualization reveals a geographically uneven research effort on the topic at hand, suggesting there is room for capacity building through international collaboration among the few places with the strongest expertise. Figure 2 shows in the inset the temporal evolution of the papers in the S-DB from 2019 to 2024 (being the number of papers published prior to 2019 almost negligible), as resulting for the DI2. A clear upward trend is evident, especially since 2020, with an exponential increase in the total number of studies. The latest year of the investigation, i.e., 2024, marks a significant peak with more than 80 papers published, indicating a rapid recent acceleration of interest in this topic, which appears to be confirmed by the 2025 trend, not addressed specifically in the analysis.

The contribution from China shows a particularly steep rise, aligning with its dominant position shown in Figure 2.

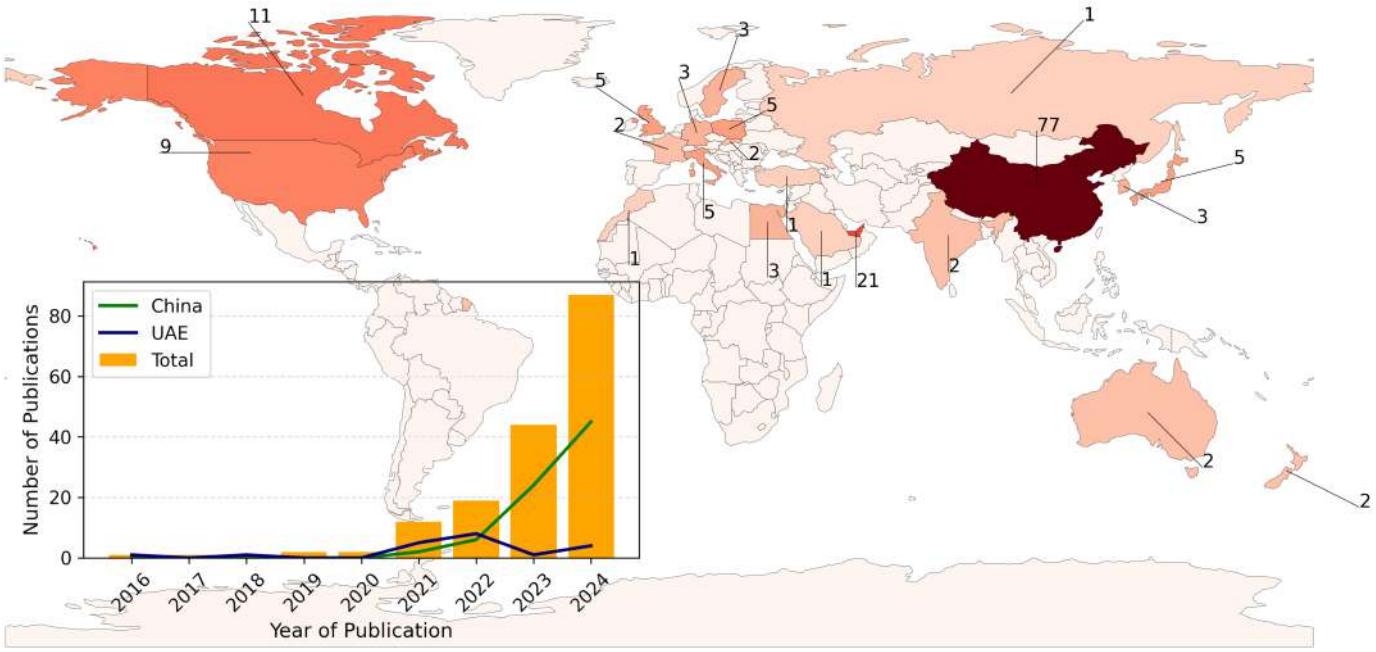

Figure 2. Distribution of the selected papers by country (DI1). The map is based on the Natural Earth data source [200]. The choice of this geographic dataset is made solely for visualization purposes and does not imply any political position or endorsement by the authors regarding territorial boundaries, sovereignty, or international relations. Inset: annual publications over the last years (DI2), with China (green) and UAE (blue) highlighted.

3.2. DI3 and DI4: Scope and Specific Application

The classification of the selected papers according to the different scopes (DI3) is reported in Figure 3, where the most common applications for TPMS lattices within the heat transfer scope (DI4) are also shown. The novelty of TPMS enables research across a broad range of topics, including flow behavior, mass transfer and absorption phenomena, and the performance of phase-change materials. As for the chosen articles, heat transfer is the main investigated aspect; this category alone represents roughly three-fourths of the total analyzed studies, as expected from the adoption of inclusion criteria IN4 and IN5 in the "Screen-and-Select" phase. Within this group, as detailed in the pie chart, the majority of contributions concern heat sinks (a), followed by heat exchangers (b), and, to a smaller extent, investigations on free convection (c) and thermo-physical material properties (d). The last category also includes studies involving PCMs, in which the main interest is evaluating the system's effective thermal conductivity. Note that the same paper can tackle two different scopes, as for instance [70,157], addressing PCM and thermo-physical properties. A minority of studies address mass transfer or absorption/adsorption problems, see for instance [56] (the only study related to two-phase flow in TPMS structures) and [169] for the first topic and [72,73,95,96] for the second.

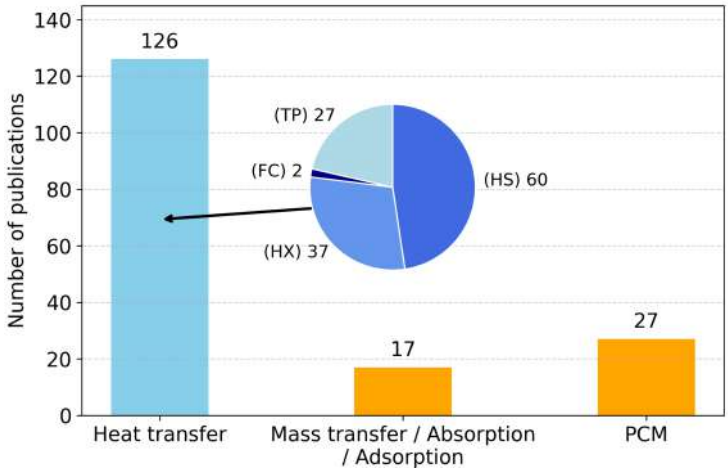

Figure 3. Distribution of the scopes addressed in the selected papers (DI3): heat transfer, mass transfer and absorption, and phase-change materials (PCMs). The pie chart details heat transfer applications (DI4): heat sinks (HSs), heat exchangers (HXs), free convection (FC), and thermo-physical (TP) properties.

3.3. DI5 and DI7: Experimental vs. Numerical Studies and Working Fluid

One of the most notable findings of this investigation concerns the focus of the study (DI5) and is illustrated in Figure 4. Over 80% of the papers rely on numerical simulations, mostly using traditional CFD, but also Lattice Boltzmann approaches. Fewer than 20 studies are based exclusively on experimental work. Almost 50 publications combine experimental measurements and numerical modeling. It is important to note, however, that reporting both experimental and numerical analyses does not necessarily imply that the numerical model was validated against the experimental data, see also DI13. Conversely, studies presenting only numerical results may still validate their findings using experimental benchmarks available in the literature. The comprehensive analysis carried out in this paper may serve both communities: it helps numerical researchers identify experimental datasets for validation, while at the same time offering experimentalists a structured overview of available numerical results that can support the design and interpretation of future tests. The experimental activity is overall dominated by investigations on HS, followed closely by HX.

A key factor influencing experimental studies on TPMS-based HS is the selection of the working fluid (DI7). As shown in Figure 4, the most commonly employed fluids are water and air, due to their cost-effectiveness, well-known thermophysical properties, and suitability for laboratory-scale testing. These fluids enable reliable measurements while keeping experimental complexity and cost relatively low. A few HS studies also consider fluids tailored to specific industrial applications, highlighting the flexibility of TPMS systems: examples include helium [162,197], supercritical CO_2 [59], and CH_4/N_2 mixtures [57].

In the context of HX, the diversity of working fluid pairs is even more pronounced. While air and water remain the most frequent experimental choices, some studies use non-standard combinations, such as air/water [130] and R134a/glycol water [120]. On the numerical side, more complex pairings have been explored, reflecting the versatility of TPMS lattices in different thermal management scenarios. These include helium/lead-bismuth eutectic (LBE) [161,166], oil with either fuel [145] or water [135], CO_2/H_2O [98] or CO_2/CO_2 [99], and acetone configurations [49]. The wide variety of fluids used in both experimental and numerical investigations raises a caveat about the comparability of results across studies. Any meaningful comparison should rely exclusively on dimensionless quantities, whose definitions must be consistent and within similar ranges among the

various works. This implies that, when analyzing heat transfer problems, not only the Reynolds number but also the Prandtl number should be comparable if any conclusions about the Nusselt number are to be drawn.

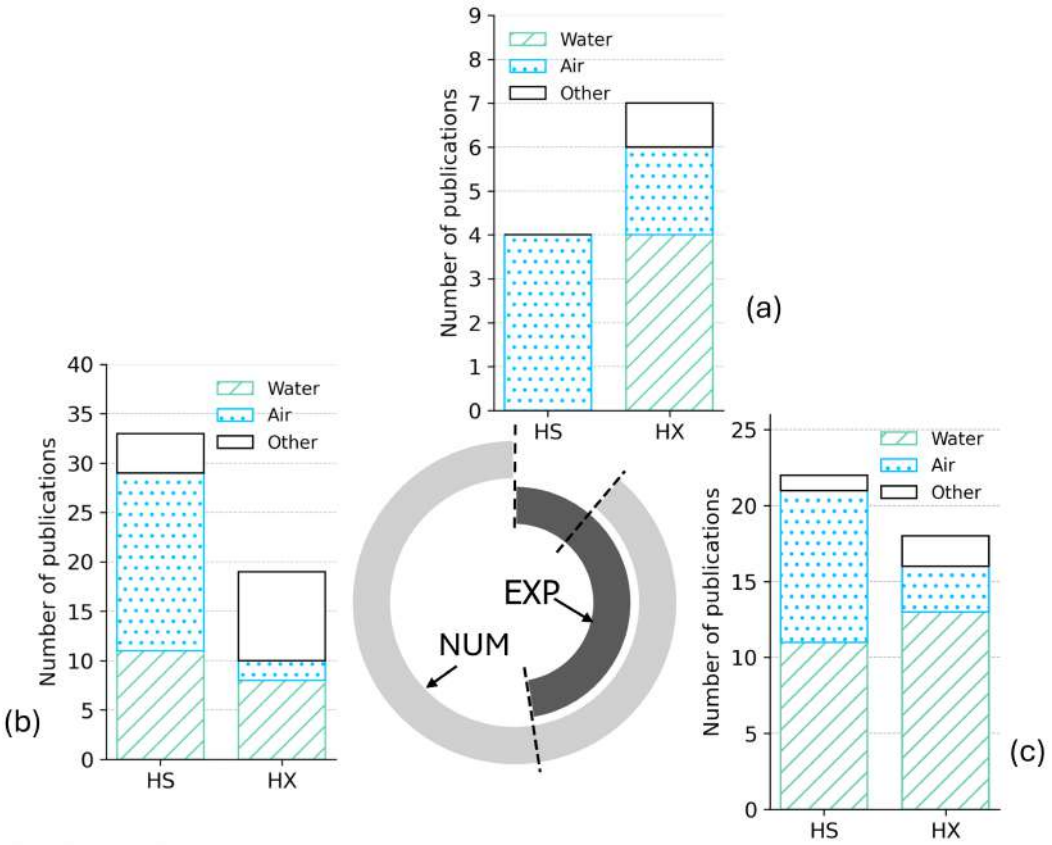

Figure 4. Distribution of the study type (DI5): experimental (EXP) or numerical (NUM). Bar plots show the heat transfer applications (HS, HX) and working fluids (DI7) for: (**a**) experimental, (**b**) numerical, and (**c**) combined studies.

3.4. DI6: Type of TPMS Generator Tool

Independently of the focus of the selected papers on experiments or numerical analyses, the generation of the TPMS lattices typically requires the use of dedicated software: the portfolio of tools adopted in the selected papers is the output of DI6, reported in Figure 5. The software MSlattice [201], developed by scholars from the UAE, is the most used in the considered papers, followed by nTop [202], which provides powerful capabilities for generating and optimizing TPMS structures. Both tools are versatile and allow the generation of highly detailed and application-specific geometries, also when functionally graded lattices are considered. MATLAB [203], which is the third most used software, offers flexibility in developing custom TPMS geometries using mathematical functions and algorithms, with the ease of integration into a well-known simulation environment. Other tools are used by a minority of the scientific community: MathMod [204], SolidWorks [205], which makes the incorporation of TPMS into mechanical components possible, Siemens NX [206], ANSYS SpaceClaim [207], the Python-based Geodict [208], Wolfram Mathematica [209], Rhinoceros [210], and others (MaSMaker [211] and LattGen [212]).

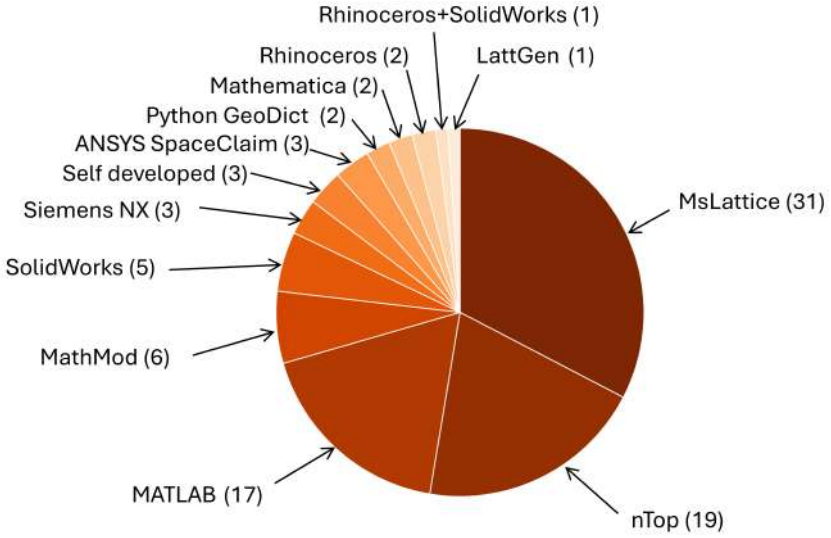

Figure 5. TPMS generation tools used in the selected papers (DI6), with the number of occurrences in brackets.

3.5. DI8: AM Methods

Figure 6 provides an overview of the AM techniques (DI8) adopted for the studies dealing with experimental tests. AM plays a crucial role in fabricating complex, highly optimized geometries such as TPMS, which are not feasible with traditional manufacturing techniques, especially for metallic items. AM processes can be classified by the type of energy source used (if any) and the materials used. Among the various AM categories, Powder Bed Fusion (PBF) is the most widely used for metallic parts. This technology creates components layer by layer by selectively fusing powdered material using a concentrated heat source. Usually, two energy sources are used, and PBF is categorized into two subgroups: Laser PBF (L-PBF) and Electron Beam PBF (EB-PBF). L-PBF is versatile, compatible with a wide range of metals and alloys. Its precision and flexibility facilitate the production of highly intricate TPMS structures, optimizing thermal performance and material efficiency [213]. L-PBF methods include: Selective Laser Sintering (SLS), Selective Laser Melting (SLM), and Direct Metal Laser Sintering (DMLS).

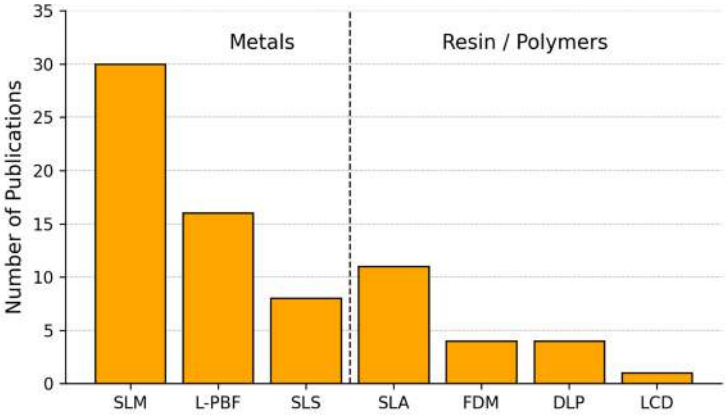

Figure 6. Additive manufacturing (AM) techniques used to fabricate samples in experimental studies (DI8).

Among PBF techniques, SLM is the most frequently used for metal devices (more than 20 papers). SLM uses a high-powered laser to melt and fuse metallic powder according to a pre-defined pattern [214]. SLS, primarily used for polymers, fuses powder particles without fully melting them [215]. It is less common for metal production compared to SLM

or DMLS as it usually results in porous or less dense parts, although some publications refer to this manufacturing technique [37,153].

While similar in process, DMLS only partially fuses metal powder. Although it excels at processing complex alloys [216], its application is very limited (only applied in [23]).

In plastic or resin manufacturing, Stereolithography (SLA) is the most widely adopted method. SLA is a photopolymerization method that employs a UV laser to cure liquid resin into solid layers. It offers high resolution and surface finish, making it suitable for producing detailed prototypes and components with fine features [217]. Its relatively low cost and compact size make SLA printers particularly suitable for research laboratories, allowing rapid design iteration and experimental testing without the need for large-scale infrastructure. Note, however, that resin may not be suitable for tests with substantial heating in view of its softening at relatively low temperatures.

Other techniques, such as Fused Deposition Modeling (FDM), Digital Light Processing (DLP), and LCD-based vat photopolymerization, are adopted in a limited number of studies. In FDM, thermoplastic filaments are extruded through a heated nozzle to build parts layer by layer. FDM belongs to the broader category called Material Extrusion, and is accessible, cost-effective, and versatile, making it popular for prototyping and low-volume production [218]. Nevertheless, it has a lower resolution than SLA, making it less suitable for TPMS applications. LCD is a vat photopolymerization technique similar to SLA but differs in its light projection methods. DLP, adopted in [149] uses a digital projector to cure entire layers simultaneously, while LCD-based 3D printing, used in [17,130], employs an LCD screen to selectively expose regions of the resin [219]. The predominance of specific additive manufacturing techniques, such as LPBF for metals and SLA for polymers, reflects a trade-off between geometric resolution, material availability, and experimental feasibility. Techniques offering higher resolution are favored in thermo-hydraulic studies, as they better preserve the designed TPMS morphology. Conversely, lower-resolution processes are mainly employed in proof-of-concept investigations, where relative performance trends are prioritized over quantitative accuracy.

3.6. DI9: Numerical Software Used for Simulation

In studies categorized as "numerical" according to DI5, the choice of the simulation software (DI9) is summarized in Figure 7. The most widely used CFD tool is ANSYS Fluent [207], appreciated for its finite volume method, user-friendly interface, and robustness in handling both laminar and turbulent regimes. Similar characteristics are offered by STAR-CCM+ [220], which is the third most adopted software. The second most used platform is COMSOL Multiphysics [221], which employs the finite element method and is mostly adopted for simulations in laminar conditions or low-Reynolds-number flows, often involving conjugate heat transfer or coupled physics problems. Open-source tools are less frequently employed: OpenFOAM [222], while powerful and highly customizable, appear in a limited number of studies. Its reduced adoption may be attributed to the steeper learning curve and, notably, to the challenges related to mesh generation, which is often more cumbersome than in commercial tools. However, this limitation can be overcome by importing meshes generated with more user-friendly software. Other software tools such as Simerics-MP+ [223] and SolidWorks Flow Simulation [205] are mentioned only in single studies, typically in turbulent regimes. Palabos [224], a Lattice Boltzmann Method (LBM) solver, is only sporadically used and mentioned here for completeness, although it is not included in the data reported in Figure 7. Despite its strengths in simulating complex boundary interactions and mesoscale transport phenomena, it has not yet gained widespread adoption within the TPMS heat-transfer community. The observed concentration of studies around a limited set of commercial CFD platforms is primarily driven by

practical rather than methodological considerations. User-friendly meshing tools, robust turbulence models, and established conjugate heat transfer capabilities make these solvers particularly attractive for handling the geometric complexity of TPMS lattices. By contrast, the limited adoption of open-source tools appears to be more closely related to meshing challenges and setup effort than to fundamental limitations in numerical accuracy.

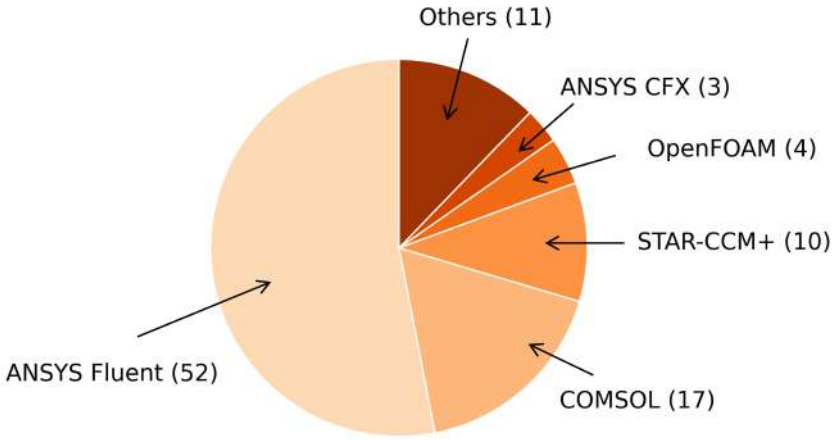

Figure 7. Simulation software adopted in CFD-based numerical investigations (DI9). The label "Others" includes numerical studies using CFD solvers different from the main software or not explicitly specified.

3.7. DI10: TPMS Topologies

A wide variety of TPMS topologies have been investigated in the S-DB papers. Each structure has distinct geometric features that influence its suitability for different heat-transfer applications. The Primitive (P), Diamond (D), and Gyroid (G) surfaces form the classical associate family of TPMS. This means that they share the same conformal structure and can be continuously transformed into one another through a simple rotation of a phase angle Φ—the Bonnet angle—in their complex Weierstrass–Enneper representation, as exemplarily shown in Figure 8. The period-closure conditions are verified for just three values of Φ (0°, 38°, and 90°), whereas all the other rotations give self-intersecting surfaces [225]. From the morphology point of view, the D lattice has a cubic Primitive (CP) structure as the Diamond in nature, whereas both the P and G lattices share a body-centered cubic (BCC) structure. However, the P lattice has mirror planes perpendicular to the cubic axes, corresponding to a non-chiral symmetry, while the G lattice features diagonal glide planes, originating a chiral geometry. This point is important because all the other topologies discussed in this study originate from one of these base surfaces (P, G, D) and consequently inherit the lattice symmetry and morphology of their parent structure. To support the interpretation of the topology-dependent trends discussed in the following sections, Table 4 provides a compact qualitative overview of the main TPMS lattice geometries considered in this review. It includes, for each topology: the sheet and solid (sometimes referred to as "network", as in [4]) variants, the two fluid domains (according to the set-level function), and the corresponding analytical expression of the level-set surface.

The Gyroid topology, as shown in Figure 9, is the most widely studied, especially in applications involving heat sinks. It is appreciated for its favorable combination of surface area, fluid accessibility, and mechanical stability, which contribute to improved heat transfer compared to conventional extended surfaces [140]. Although HS dominates its application domain, several studies have also successfully explored its use in HX.

The Diamond lattice is the second most investigated structure and shares several performance similarities with the G topology. In particular, both are especially suitable for HX configurations, as they divide the domain into two self-complementary fluid regions

when implemented in the sheet variant. This geometric peculiarity, also shared by several other TPMS in Table 4, facilitates the design of balanced HX configurations. Note, however, that, as opposed to the Gyroid topology, the Diamond topology is achiral. The dominance of Gyroid and Diamond topologies in HS and HX applications (see Figure 9) is not accidental, but can be traced back to a combination of geometric and functional factors. Both structures offer a favorable compromise between surface-to-volume ratio and permeability, while their smooth curvature limits localized pressure losses. Moreover, in their sheet variants, Gyroid and Diamond lattices generate two continuous fluid domains, a property that significantly simplifies the design of compact heat exchangers compared to non-self-complementary TPMS. These features explain why, despite the availability of many alternative TPMS geometries, the literature remains strongly polarized toward these two topologies.

The Primitive topology is characterized by a regular and open geometry that facilitates fabrication and flow. It produces two identical domains and is occasionally employed in HS or HX studies. However, its high permeability and relatively low surface area make it more suited to low-resistance applications, such as filters, which fall outside the scope of this investigation.

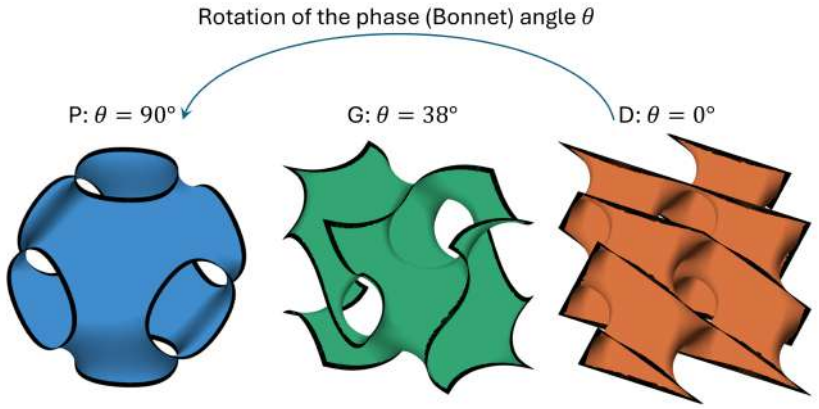

Figure 8. Sketch of the phase rotation to move from D to G to P topologies.

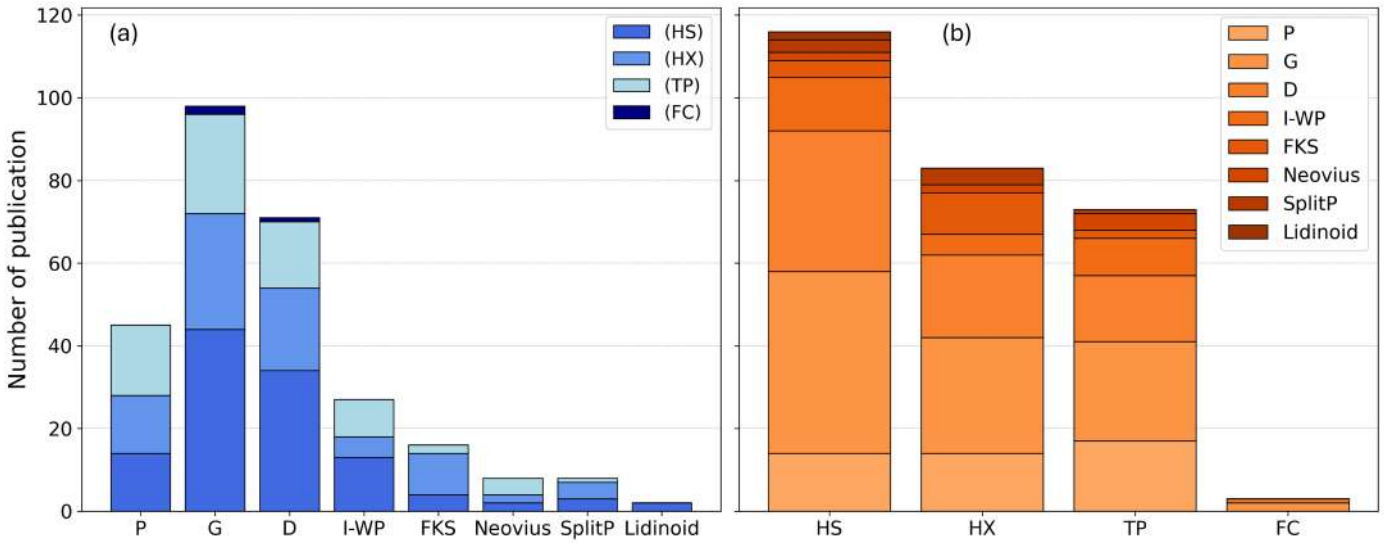

Figure 9. Distribution of publications by TPMS topology and application scope (DI10). Stacked bars show: (**a**) topologies by application of heat transfer and (**b**) application by topology. Applications include Heat Sinks (HSs), Heat Exchangers (HXs), Free Convection (FC), and thermo-physical (TP) properties.

Table 4. Overview of the main TPMS topologies considered in this study, including their solid and sheet representations, the corresponding fluid domains generated by the level-set formulation, and the analytical expressions of the implicit surfaces. The table is intended as a qualitative reference to support the interpretation of topology-dependent trends discussed in Sections 3 and 4, rather than as a performance comparison. For clarity, only the most commonly adopted TPMS in thermal applications are reported.

Topology	Solid	Sheet	Fluid 1	Fluid 2	Set-Level Function
Primitive			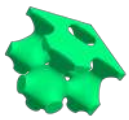	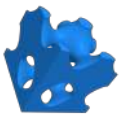	$\cos(X)+\cos(Y)+\cos(Z)=0$
Gyroid			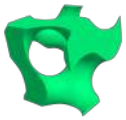		$\sin(X)\cos(Y)+\sin(Y)\cos(Z)+$ $\sin(Z)\cos(X)=0$
Diamond				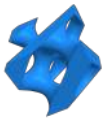	$\sin(X)\sin(Y)\sin(Z)+\sin(X)\cos(Y)\cos(Z)+\cos(X)\sin(Y)\cos(Z)$ $+\cos(X)\cos(Y)\sin(Z)=0$ $\cos(X)\sin(Y)\cos(Z)-\sin(X)\sin(Y)\sin(Z)=0$
I-WP					$\cos(X)\cos(Y)+\cos(Y)\cos(Z)+$ $\cos(Z)\cos(X)-\sin(X)\sin(Y)\sin(Z)=0$
FKS			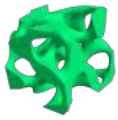	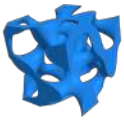	$\cos(2X)\sin(Y)\cos(Z)+$ $\cos(X)\cos(2Y)\sin(Z)+$ $\sin(X)\cos(Y)\cos(2Z)=0$
Neovius			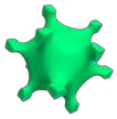	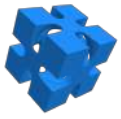	$3(\cos(X)+\cos(Y)+\cos(Z))+$ $4\cos(X)\cos(Y)\cos(Z)=0$
SplitP			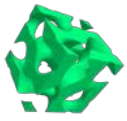	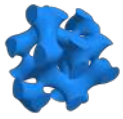	$1.1(\sin(2X)\sin(Z)\cos(Y)+\sin(2Y)\sin(X)\cos(Z)+\sin(2Z)\sin(Y)\cos(X))$ $-0.2(\cos(2X)\cos(2Y)+\cos(2Y)\cos(2Z)+\cos(2Z)\cos(2X))$ $-0.4(\cos(2X)+\cos(2Y)+\cos(2Z))=0$
Lidinoid *			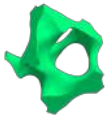	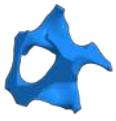	$\sin(2X)\cos(Y)\sin(Z)+\sin(2Y)\cos(Z)\sin(X)+\sin(2Z)\cos(X)\sin(Y)$ $-\cos(2X)\cos(2Y)-\cos(2Y)\cos(2Z)-\cos(2Z)\cos(2X)+0.3=0$

* A third hydraulic channel opens up for porosities greater than 50%, depending also on the wall thickness.

The I-WP structure is recognized for its smooth morphology and high interconnectivity. While its mechanical and flow characteristics are advantageous, the two regions generated by the level-set function are not self-complementary, making its direct application in heat exchangers less straightforward. Nonetheless, it has been explored in advanced applications such as catalytic reactors and microscale exchangers [161,166,179]. From a morphology standpoint, the I-WP surface is D-related, sharing the same CP lattice as the Diamond surface but with a lower symmetry. This symmetry reduction results in two morphologically distinct labyrinths, in contrast to the self-complementary nature of the parent D surface.

The Fischer–Koch S (FKS) lattice introduces a higher level of geometric complexity while preserving domain symmetry. Its intricate surfaces result in elevated area-to-volume ratios and have been employed in the design of compact micro-heat exchangers and energy storage devices [120,135,162,165]. From a geometrical standpoint, the FKS surface belongs to the D-related family and shares the same CP lattice as the D surface. Its symmetries allow the two hydraulic regions to remain self-complementary when in sheet form. Compared to the D surface, the FKS displays a higher topological complexity and a smoother curvature distribution, offering enhanced isotropy and diffusion uniformity within the pore network.

The Neovius topology is rarely adopted but remains of interest due to its modular, periodic geometric structure, which could be exploited in microreactors or compact heat exchangers. In its sheet variant, it gives origin to non-self-complementary channels, despite sharing the overall cubic symmetry with the P surface. From a morphological standpoint, the Neovius surface shares the same BCC lattice as the P surface and is therefore achiral.

The SplitP and Lidinoid structures have been analyzed in fewer studies. The Split-P topology generates fluid domains with significantly different shapes and volumes, posing challenges for heat-exchanger design where balanced flow distribution is required. This asymmetry arises from partial breaking of the P-surface symmetry, producing two morphologically distinct regions separated by a single continuous interface. When it is in the solid variant, the difference between the two regions requires choosing which one to print as solid, whereas in the sheet variant, it requires careful consideration. The Lidinoid lattice, instead, can be regarded as a non-chiral analogue of the Gyroid and yields two equivalent and spatially shifted channels. Interestingly, at certain porosities (above >50%, also depending on the wall thickness), the Lidinoid sheet evolves from a bicontinuous to a tricontinuous topology, where a third disconnected fluid region emerges within the structure. This additional domain limits design flexibility and complicates manufacturing. Also, when this third region is discontinuous, it may introduce isolated cavities that impede complete fluid percolation and a uniform coating during fabrication processes.

Finally, topologies such as FRD, W-Type, Koch, and C, as well as some hybrid configurations, are reported only in isolated studies and are not included in Table 4. These geometries have been primarily explored to assess their thermal performance in comparison to better-known TPMS types. While promising in certain cases, they do not yet provide a consolidated reference for design and optimization in heat-transfer applications and fall outside the current focus of this investigation.

3.8. DI11: Flow Regime Investigated

The multi-ring donut chart in Figure 10 provides an integrated view of the flow regime investigated (DI11) across the different papers, linked to the focus of the study (DI5) and the specific application (DI4).

Most experimental studies focus on the turbulent regime, particularly for HS and HX applications, with a strong emphasis on Gyroid and Diamond structures. Laminar flow conditions, on the other hand, are seldom explored experimentally, likely due to the need for more sensitive and precise instrumentation to capture low-velocity fields. From a numerical perspective, approximately 30% of studies simulate laminar flows, primarily in the context of HS applications, where Gyroid topologies predominate. Turbulent flow remains the dominant regime overall, reflecting its relevance to industrial conditions, especially for HX. In most HX studies, topologies with self-complementary channels are adopted, as expected. In the case of HS, the number of laminar and turbulent studies is more balanced, due to the growing interest in low-Reynolds applications such as microelectronics cooling [36].

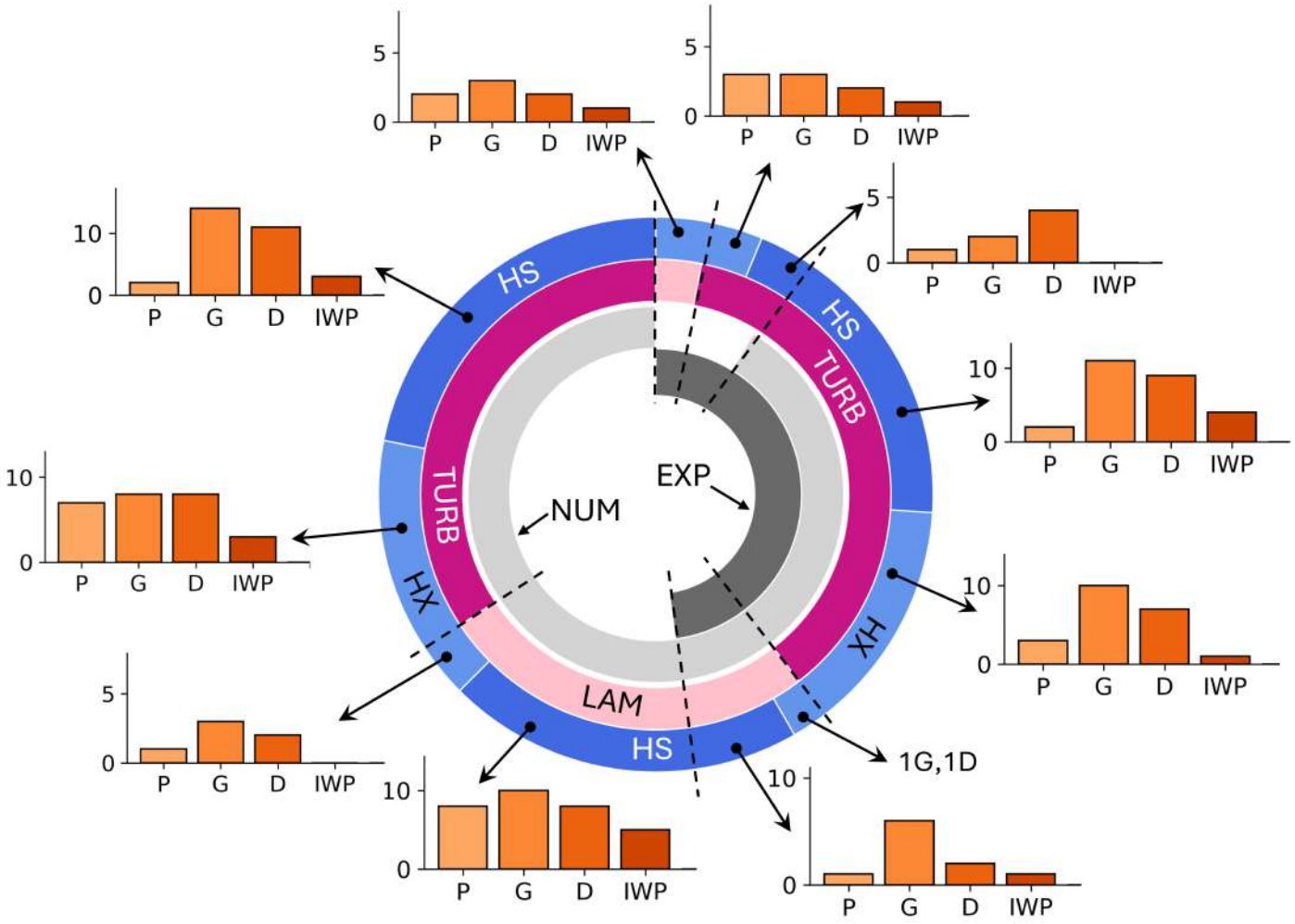

Figure 10. Flow regimes investigated (DI11), cross-referenced with study type (DI5) and application (DI4), specifically HS and HX. For other applications, the most common TPMS topologies (DI10) are shown in the bar plots.

The strong emphasis on turbulent flow conditions observed in the literature reflects the intended alignment with industrial operating regimes rather than a lack of interest in laminar configurations. Turbulent studies allow direct comparison with conventional heat transfer devices and facilitate the use of established performance metrics. By contrast, laminar regimes are primarily explored in numerical studies, where low-Reynolds-number conditions can be investigated without the experimental challenges of precise flow and temperature measurements.

Note that each study in Figure 10 can belong to more than one subcategory, according to its content. For instance, in [65] HS are investigated, both numerically and experimentally, in the laminar and turbulent regimes, but the number of such examples is quite limited.

3.9. DI12: Turbulence Closures

In numerical studies, researchers are increasingly focusing on identifying the most suitable turbulence closure models to address the complex flow structures typical of TPMS geometries. The relationships between the adopted flow regime (DI11), simulation software (DI9), and turbulence models (DI12) are summarized in Figure 11.

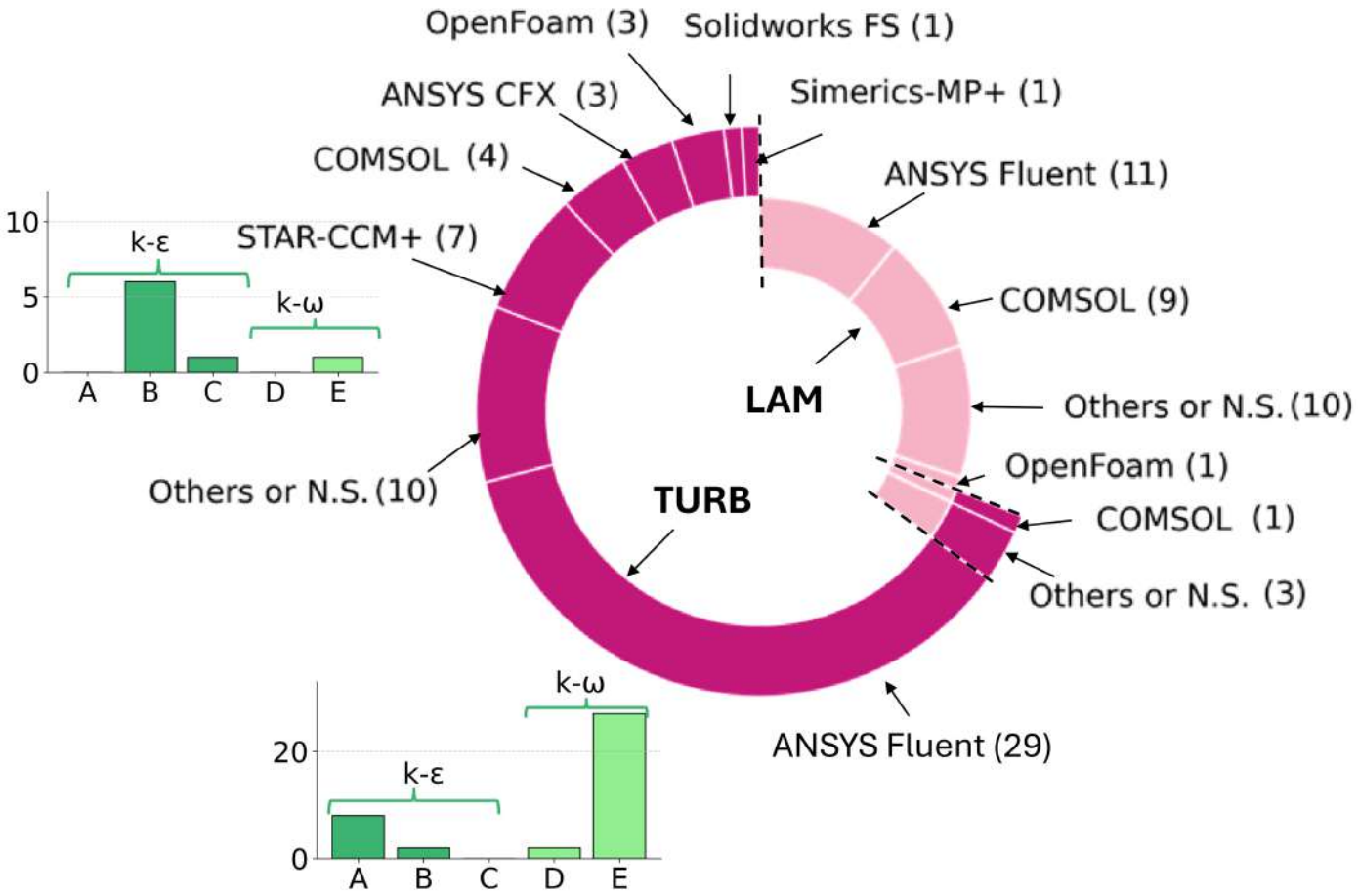

Figure 11. Overview of the simulation tools and turbulence modeling approaches. Outer ring: distribution of simulation software in laminar (LAM) and turbulent (TURB) regimes (DI9 and DI11). Bar charts: turbulence models used in the selected papers (DI12), grouped into the *k*-ε family (A = standard, B = Realizable, and C = lag EB) and the *k*-ω family (D = standard, E = SST).

All turbulent simulations in the reviewed studies adopt Reynolds-Averaged Navier–Stokes (RANS) models for turbulence closure. No papers investigate Large Eddy Simulation (LES) or Direct Numerical Simulation (DNS).

The two-equation Standard *k*-ε model is a well-established and widely implemented RANS approach. Despite its widespread implementation in commercial and open-source CFD codes, it is used in a limited number of studies, mainly those employing Fluent, COMSOL, and Simerics-MP.

The Realizable *k*-ε model, a refinement of the standard formulation, is designed to improve accuracy in flows with strong curvature, separation, or rotation [226]. It is preferred by research groups using STAR-CCM+, where its numerical robustness is particularly appreciated. A single study also applies the Lag Elliptic-Blending *k*-ε variant [74], following promising performance previously observed in simplified geometries [227].

The Standard *k*-ω model, known for its improved near-wall resolution [228], is used in a few studies with Fluent [104,146]. More commonly, the *k*-ω SST (Shear Stress Transport) model [229] is adopted, especially within Fluent-based investigations, due to its proven reliability in predicting separated flows.

Interestingly, the authors of [88] report that in some test cases involving Gyroid and Diamond structures, the Standard *k*-ε model provided better agreement with experimental data compared to the more advanced *k*-ω SST formulation.

The exclusive adoption of RANS turbulence closures observed in the reviewed literature is primarily driven by computational constraints rather than by physical considerations.

TPMS geometries induce strong curvature-driven secondary flows and local recirculation, which are known to challenge eddy-viscosity models. However, the short computational domains typically employed (often limited to a few unit cells), and the high cost associated with LES or DNS for full devices have so far discouraged higher-fidelity approaches. As a result, turbulence modeling choices are often pragmatic rather than rigorously validated.

3.10. DI13: Validation of the Numerical Models

While solution verification, such as grid independence studies or uncertainty estimation via the Grid Convergence Index (GCI) method (as done, for example, in [26]), is commonly reported in the analyzed studies, the validation of numerical models against experimental results is a less standardized practice.

To better quantify this aspect, the numerical papers were classified based on whether they include original or external experimental data (i.e., if they also included an experimental part, EXP), and, if so, whether a direct comparison with the numerical results (i.e., a form of "validation") is provided, as summarized in Figure 12. Out of the 112 heat-transfer papers that include numerical simulations, 66 are purely numerical, and almost 50 combine experiments and simulations. Validation against experimental data is performed in two-thirds of the combined experimental–numerical studies and, suprisingly, in half of the purely numerical studies, using as a reference external data from the literature. While several studies report qualitative agreement between simulations and experiments (e.g., trend consistency or visual comparison), only a limited subset performs quantitative validation with explicit error metrics or uncertainty bounds. Validation practices also depend on the application domain. Studies focused on heat exchangers can easily include experimental benchmarks, as HX performance is often assessed through integral quantities that are easier to measure experimentally. In contrast, heat sink studies commonly rely on localized thermal metrics, which are more challenging to validate experimentally. From a topological perspective, Gyroid and Diamond lattices benefit from a broader experimental basis, which explains their frequent use as reference geometries in numerical benchmarking, whereas less common TPMS topologies are often investigated without direct experimental validation. Therefore, while formal validation procedures remain relatively rare, more than half of all numerical studies include some form of comparison with experimental results. This underscores the growing but still incomplete effort to anchor simulations to physical measurements, whether obtained by the same authors or retrieved from existing benchmarks. Note that validation is revisited in Section 5 as a central element for assessing the robustness of reported performance trends and correlations.

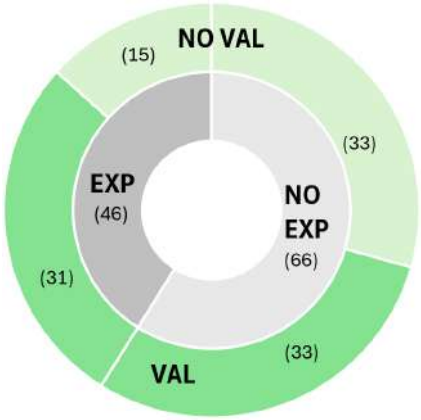

Figure 12. Validation practices in numerical studies (DI13). Inner ring: studies including (EXP) or not including (NO EXP) experimental data. Outer ring: presence (VAL) or absence (NO VAL) of comparison between simulations and experiments.

4. Use of the S-DB to Analyze Gyroid and Diamond HS and HX

4.1. Studies on Heat Sinks

The publications dealing with HS applications are synthesized in Figure 13. The central pie chart shows the share of TPMS topologies used as heat sinks (DI10), highlighting the dominance of Gyroid and Diamond structures. The two sunburst plots on the sides provide additional insight into these two topologies by, for each working fluid (DI7), resolving the flow regime (DI11) and the type of study (DI5). In combination with the detailed information reported in Tables 5 and 6, this figure shows that most HS-oriented investigations rely on air-cooled devices operating in turbulent conditions and are primarily based on numerical simulations, with experimental work limited to a smaller number of contributions.

Table 5. Publications on HS, involving Gyroid topology.

DOI	Fluid	Type of Study	Validation	Flow Regime	Turb. Model	Sim. Software
[118]	Air	EXP	–	TURB	–	–
[177]	Air	EXP	–	TURB	–	–
[152]	Air	EXP, NUM	–	LAM + TURB	–	–
[151]	Air	EXP, NUM	–	TURB	*k-ω* SST	–
[81]	Air	EXP, NUM	X	TURB	Standard *k-ε*	ANSYS Fluent
[44]	Air	EXP, NUM	X	TURB	*k-ω* SST	ANSYS Fluent
[45]	Air	EXP, NUM	X	TURB	*k-ω* SST	ANSYS Fluent
[153]	Air	EXP, NUM	X	TURB	*k-ω* SST	ANSYS Fluent
[88]	Air	EXP, NUM	X	TURB	Realizable *k-ε*, *k-ω* SST	STAR-CCM+
[58]	Air	NUM	–	LAM	–	ANSYS Fluent
[40]	Air	NUM	X	LAM	–	ANSYS Fluent
[34]	Air	NUM	–	TURB	Realizable *k-ε*	STAR-CCM+
[47]	Air	NUM	–	TURB	Standard *k-ε*	SolidworksFS
[66]	Air	NUM	X	TURB	*k-ω* SST	ANSYS Fluent
[77]	Air	NUM	X	TURB	*k-ω* SST	ANSYS Fluent
[140]	Air	NUM	X	TURB	*k-ω* SST	ANSYS Fluent
[192]	Air	NUM	X	TURB	*k-ω* SST	ANSYS Fluent
[110]	Air	NUM	X	TURB	Realizable *k-ε*	STAR-CCM+
[183]	Air	NUM	X	TURB	Realizable *k-ε*	COMSOL
[188]	Air	NUM	X	TURB	Realizable *k-ε*	COMSOL
[197]	He	NUM	X	LAM	–	ANSYS Fluent
[57]	$CH_4 + N_2$	NUM	–	LAM	–	ANSYS Fluent
[158]	N_2	EXP, NUM	X	TURB	Standard *k-ε*	ANSYS Fluent
[59]	SCO_2	NUM	–	LAM	–	ANSYS Fluent
[65]	Water	EXP, NUM	–	LAM + TURB	–	COMSOL
[54]	Water	EXP, NUM	X	LAM	–	COMSOL
[133]	Water	EXP, NUM	X	LAM	–	COMSOL
[134]	Water	EXP, NUM	X	LAM	–	COMSOL
[93]	Water	EXP, NUM	X	TURB	Standard *k-ε*	ANSYS Fluent
[190]	Water	EXP, NUM	X	TURB	*k-ω* SST	–
[137]	Water	EXP, NUM	X	–	–	COMSOL
[36]	Water	NUM	X	LAM	–	ANSYS Fluent
[80]	Water	NUM	X	LAM	–	ANSYS Fluent
[87]	Water	NUM	X	LAM	–	ANSYS Fluent
[127]	Water	NUM	X	LAM	–	ANSYS Fluent
[46]	Water	NUM	–	TURB	*k-ω* SST	ANSYS Fluent
[61]	Water	NUM	–	TURB	*k-ω* SST	ANSYS Fluent
[74]	Water	NUM	–	TURB	lag EB *k-ε*	STAR-CCM+
[121]	Water	NUM	–	TURB	Realizable *k-ε*	STAR-CCM+
[171]	Water	NUM	X	TURB	*k-ω* SST	ANSYS Fluent

Table 5. *Cont.*

DOI	Fluid	Type of Study	Validation	Flow Regime	Turb. Model	Sim. Software
[138]	Water	NUM	X	–	–	COMSOL
[136]	Water+Nanoparticles	EXP, NUM	X	–	–	COMSOL
[169]	–	NUM	–	LAM	–	–
[172]	–	NUM	–	LAM	–	COMSOL
[111]	–	NUM	–	–	–	–

Table 6. Publications on HS, involving diamond topology.

Ref	Fluid	Type of Study	Validation	Flow Regime	Turb. Model	Sim. Software
[118]	Air	EXP	–	TURB	–	–
[177]	Air	EXP	–	TURB	–	–
[51]	Air	EXP	–	TURB	–	–
[114]	Air	EXP	–	TURB	–	–
[152]	Air	EXP, NUM	–	TURB + LAM	–	–
[44]	Air	EXP, NUM	X	TURB	k-ω SST	ANSYS Fluent
[45]	Air	EXP, NUM	X	TURB	k-ω SST	ANSYS Fluent
[88]	Air	EXP, NUM	X	TURB	Realizable k-ε + k-ω SST	STAR-CCM+
[175]	Air	EXP, NUM	X	TURB	Standard k-ε	ANSYS Fluent
[176]	Air	EXP, NUM	X	TURB	Standard k-ε	–
[42]	Air	NUM	–	LAM	–	OpenFoam
[58]	Air	NUM	X	LAM	–	ANSYS Fluent
[34]	Air	NUM	–	TURB	Realizable k-ε	STAR-CCM+
[187]	Air	NUM	X	TURB	k-ω SST	ANSYS Fluent
[192]	Air	NUM	X	TURB	k-ω SST	ANSYS Fluent
[184]	Air	NUM	X	TURB	k-ω SST	ANSYS Fluent
[77]	Air	NUM	X	TURB	k-ω SST	ANSYS Fluent
[186]	Air	NUM	X	TURB	Realizable k-ε	ANSYS Fluent
[188]	Air	NUM	X	TURB	Realizable k-ε	COMSOL
[185]	Air	NUM	X	TURB	Realizable k-ε	COMSOL
[110]	Air	NUM	X	TURB	Realizable k-ε	STAR-CCM+
[57]	CH_4 + N_2	NUM	–	LAM	–	ANSYS Fluent
[158]	N_2	EXP, NUM	X	TURB	Standard k-ε	ANSYS Fluent
[59]	SCO_2	NUM	–	LAM	–	ANSYS Fluent
[143]	Water	EXP, NUM	–	LAM	–	ANSYS Fluent
[93]	Water	EXP, NUM	X	TURB	Standard k-ε	ANSYS Fluent
[190]	Water	EXP, NUM	X	TURB	k-ω SST	–
[80]	Water	NUM	X	LAM	–	ANSYS Fluent
[127]	Water	NUM	X	LAM	–	ANSYS Fluent
[121]	Water	NUM	–	TURB	Realizable k-ε	STAR-CCM+
[171]	Water	NUM	X	TURB	k-ω SST	ANSYS Fluent
[138]	Water	NUM	X	–	–	COMSOL
[172]	–	NUM	–	LAM	–	COMSOL
[169]	–	NUM	–	LAM	–	–

In the following, we do not aim at an exhaustive description of the thermal performance reported in each contribution, which would be hardly comparable because of the different operating ranges and performance indicators adopted. Instead, we emphasize, for each cluster of studies, the most relevant geometrical choices, modeling strategies, and performance metrics that will be critically discussed in Section 5, with the goal of identifying robust trends and current gaps in the literature.

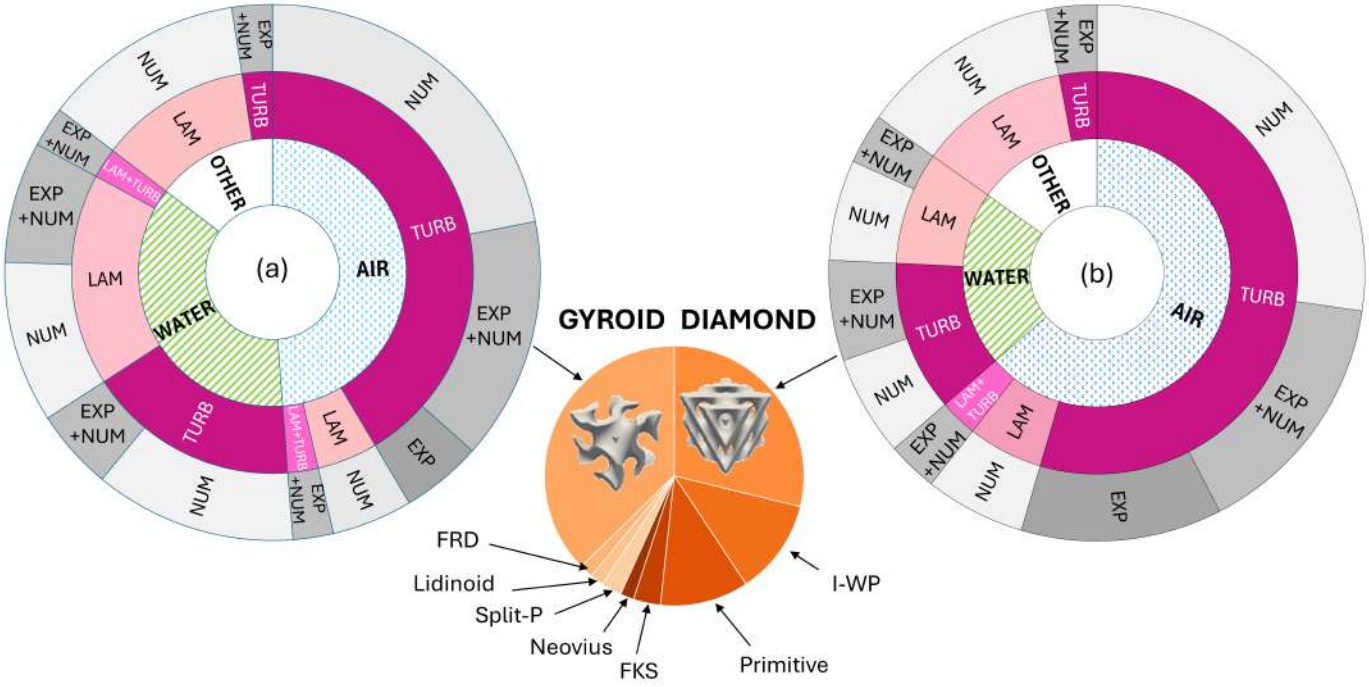

Figure 13. Distribution of the results for the Data Item DI10, for the papers relative to HS (Pie chart). The details on the flow regime (DI11) and type of study (DI5) for the different operating fluids (DI7) investigated in the studies involving G (**a**) and D (**b**) lattices are also reported.

4.1.1. Gyroids with Air as the Working Fluid

As already anticipated by Figure 13a, Gyroid-based heat sinks cooled by air constitute the most extensively explored configuration, and their main features are summarised in Table 5. The body of work can be broadly grouped into (i) laminar studies on idealised or customised lattices, often with a strong geometrical-design flavour, and (ii) turbulent studies on more application-oriented channels, where attention is shifted towards manufacturability and system-level performance.

Only two contributions address purely laminar air flow through Gyroid structures, both by means of numerical simulations [40,58]. In [40], recognizing the enhanced mixing promoted by TPMS, a two-dimensional lattice of polygons is mapped onto a Gyroid sheet, thereby generating a surface tessellation. The study explores the effect of polygon shape and size on the flow and heat transfer in pipes filled with such structures for $1 \leq \mathrm{Re} \leq 200$. In [58], a design-oriented methodology is proposed to customise solid TPMS (Gyroid, Diamond, I-WP and Primitive) over a wide porosity range (0.2–0.8), using a domain consisting of a row of eight lattice cells and Reynolds numbers from 10 to about 130. The thermal–hydraulic performance is compared using the ratio between the Colburn and friction factors (referred to by the authors as an "area goodness factor"), and the I-WP lattice is identified as the best performing topology under the investigated laminar conditions. Interestingly, while the lattice is clearly identified as a porous medium, which could hint at a Darcy–Forchheimer framework as done, for instance, in [230], the heat-transfer analysis relies on classical Nusselt-type correlations. This sort of internal inconsistency between momentum and heat-transfer models will be revisited in Section 5.

A mixed laminar–turbulent configuration is examined in [152], where sheet Gyroid, Diamond, and I-WP lattices with identical cell size and thickness are 3D-printed as four cells in a row on a heated surface. The study couples experiments and simulations across a Reynolds-number range spanning both regimes, and includes a comparison between numerical and measured pressure-drop data for the Gyroid case. Based on their analysis, the authors conclude that the Diamond lattice achieves the highest convective heat-transfer

performance. However, the influence of entry-region effects and the streamwise extent required to reach fully developed flow are not systematically assessed.

When these two contributions are considered together, a clear discrepancy emerges. Under comparable Reynolds-number ranges and using nominally similar metrics, [58] reports the I-WP lattice as the most effective topology, while [152] identifies the Diamond lattice as the superior performer. These conflicting conclusions stem from several factors: (i) the adoption of different performance metrics, which are not standardised for TPMS and may emphasize different aspects of the thermal–hydraulic response; (ii) differing levels of experimental benchmarking and numerical model validation; (iii) variations in the treatment of developing-flow regions, which are known to affect both Nusselt number estimates and friction factors. This lack of methodological uniformity across studies makes it difficult to derive robust rankings of TPMS topologies and underscores the need for harmonised evaluation practices, as discussed in Section 5.

The majority of studies on air-cooled Gyroid HS focus on turbulent flow and are dominated by channel configurations containing a limited number of unit cells. A numerical work in this direction is [34], where Gyroid solid and sheet lattices arranged as $2 \times 2 \times 4$ cells are inserted in a square channel heated on all sides. The Gyroid sheet provides the highest heat transfer coefficient at the expense of a substantial pressure drop, and the feasibility of 3D printing and graded lattices is discussed. Building on the concept of grading and mapping, the topology–optimization study [110] compares graded and uniform Gyroid and Diamond lattices (both sheet and solid) in a one-sided heated square channel containing a $2 \times 2 \times 2.5$ lattice region. Based solely on the CFD results, the Diamond-sheet configuration is reported as providing the most favorable balance between heat-transfer enhancement and pressure loss.

However, these numerically derived conclusions do not fully align with available experimental evidence. In particular, the campaign presented in [177], conducted in a comparable Reynolds-number range ($\mathrm{Re} \approx 500$–1000), shows that the Gyroid-sheet lattice exhibits a higher ratio of the Chilton–Colburn factor to the friction factor than the Diamond-sheet lattice. This divergence highlights a broader issue already observed in the literature: the performance assessment of TPMS structures relies on heterogeneous and often non-equivalent evaluation criteria, which are not yet standardized for porous-like architectures.

Several works further explore the thermal-hydraulic behavior of Gyroid heat sinks in similar square-channel arrangements, often using four to five cells in the streamwise direction, and adopting different RANS closures. For instance, [88] investigates Gyroid sheet and solid lattices, along with a Diamond-solid configuration, in the range $2000 \leq \mathrm{Re} \leq 6000$, and compares experimental and numerical pressure drops. Good agreement is obtained when the Realizable k-ε model is employed, and performance is ranked using the Performance Evaluation Criterion (PEC) proposed in [231] at fixed pumping power, which leads to the Diamond solid lattice being identified as the most efficient solution. The suitability and practical implementation of such a PEC for TPMS lattices, however, are not straightforward, as they require a consistent definition of an equivalent smooth channel and of the characteristic velocity; this aspect will be addressed in the general discussion.

On the experimental side, [118,177] provide important benchmarks for turbulent-flow in air-cooled Gyroid heat sinks. In [118], Gyroid-sheet and Diamond-sheet lattices manufactured from polymer and subject to volumetric heating are tested for $500 \leq \mathrm{Re} \leq 6500$. Local measurements indicate that the Nusselt number remains almost constant along the streamwise direction, suggesting that reliable average correlations can be formulated. In [177], aluminium Gyroid, Diamond, and Primitive sheet lattices (including hybrid combinations) are tested, and the measured porosity is found to be lower than the CAD value,

emphasizing the impact of manufacturing on the effective geometric parameters. Among the tested topologies, the Gyroid exhibits the lowest pressure drop.

Several recent numerical studies use these experimental datasets to evaluate turbulence models and explore more advanced geometric modifications. Examples include the comparison between plane Gyroid-sheet lattices and variants equipped with surface fins [151], and the investigation of cell-size effects for different porosities and materials [140]. Other works introduce controlled deformations of the Gyroid surface [44,153] or more peculiar modifications and alternative TPMS such as SplitP and Lidinoid [45]. In all these contributions, the k-ω SST model is typically adopted and validated against a subset of experimental cases, with varying levels of agreement, which again points to the need for a more quantitative and systematic model assessment.

Finally, some studies depart from the standard straight-channel geometry and address configurations closer to technological applications. For example, wedge-shaped channels representative of turbine blade cooling are analyzed [77] or in [188], where Gyroid, Diamond, and I-WP sheet and solid lattices are compared over $10^4 \leq \mathrm{Re} \leq 3 \times 10^4$. The Diamond sheet is reported to provide the best trade-off between heat transfer enhancement and pressure loss relative to pin-fin baselines, and the impingement and mixing induced by Gyroid and Diamond sheets are highlighted as the main mechanisms controlling the heat transfer. The influence of lattice rotation around an axis normal to the heated surface is explored in [192] using a reduced computational domain, and the resulting PEC (again based on [231]) is shown to be highly sensitive to the rotation angle, which is proposed as a practical design knob. The rotation of the lattice is claimed to be a good trick for tailoring the structural efficiency to the desired value. Note, however, that a complete rotation in 3D, also involving the axis parallel to the heated surfaces, has not been addressed so far and deserves attention.

Overall, the literature on Gyroid heat sinks with air reveals a number of recurring features: simulations are often confined to short lattice rows, with limited discussion of entrance effects and of the establishment of fully developed conditions; different definitions of Reynolds number and characteristic velocity are adopted; and a variety of performance indicators (in particular, different implementations of PEC) are used. These aspects, together with the porous-medium analogy and the choice of turbulence models, are revisited and critically assessed in Section 5.

4.1.2. Gyroids with Water as the Working Fluid

Studies employing water as the working fluid cover a wider range of operating conditions than those using air, and several contributions explicitly include laminar configurations. A representative example is [80], in which a square channel with two unit cells in a row is analyzed with one heated wall. Both Gyroid-sheet and Diamond-sheet lattices are considered, together with a progressive stretching of the cells along the flow direction. The stretching reduces the pressure drop with only a mild penalty on heat transfer. The performance ranking is again expressed through the PEC, and the Diamond Sheet lattice emerges as the most efficient solution within the tested range.

A full-scale HS configuration is analyzed in [36], where a single layer of Gyroid-sheet cells is used for microprocessor cooling. Different porosities and loading conditions are explored, and a comparison with pin-based geometries highlights the advantages of TPMS-enhanced mixing. A similar problem is addressed in [54] through both experiments and simulations, with comparable conclusions. Further considerations on electronics cooling are discussed in [93], which focuses on graded Gyroid-solid and Diamond-solid lattices. The proposed structures are shown to provide a viable alternative to straight channels by combining mixing enhancement and acceptable pressure losses.

Another important application is reported in [61], dealing with the optimization of a cold-plate configuration. Here, a Gyroid lattice with trimmed thickness is used to guide the flow through a U-shaped path. A parametric study of key geometric variables enables the identification of an optimised configuration that outperforms a serpentine cooling strategy in heat transfer.

More recent literature extends the adoption of TPMS to cooling strategies for high-heat-flux components in nuclear fusion systems. In [74], Gyroid-sheet, Gyroid-solid, and SplitP-sheet metallic structures are proposed for the cooling of mirrors in the microwave transmission lines for plasma heating. All examined topologies are shown to satisfy the design constraints. In [121], a Gyroid-sheet lattice is used to design a divertor tile for the Wendelstein 7-X stellarator, withstanding heat loads up to $10\,\mathrm{MW/m^2}$.

A more fundamental perspective on thermal transport mechanisms is presented in [133], which compares experimentally and numerically a metal foam and a Gyroid-sheet lattice as porous cooling media. The Gyroid structure exhibits a consistently higher PEC, thus pointing towards a more favorable interplay between mixing and pressure losses. The same research group extends the analysis in [134], introducing an impinging-jet cooling configuration and exploring different lattice porosities. The effect of cell size and porosity is further investigated in [65] using the same experimental setup.

Beyond these canonical geometries, the work in [93] evaluates the thermal-hydraulic performance of several TPMS, including Gyroid, Diamond, Primitive, and the more unconventional FRD topology. The authors propose a useful representation of the performance in the $(\mathrm{Nu},\ \xi)$ plane, where ξ is a pressure-drop coefficient. This two-parameter space allows a straightforward visual selection of the most suitable topology for a given application. In analogy to the recursive Gyroid studied for air in [47], the analysis in [46] shows that recursive configurations may help alleviate the pressure-drop penalty typically associated with TPMS.

As a final remark, two additional contributions mostly devoted to structural optimization, [111,169] are not included in Figure 13a. These works rely on idealized, non-heated, or highly reduced domains and therefore fall outside the scope of this subsection.

4.1.3. Diamonds with Air and Water as the Working Fluids

The sunburst plot in Figure 13b shows that most Diamond-based HS studies involve air-cooled devices operating in turbulent conditions. Four contributions are purely experimental, whereas several other works combine numerical simulations and test data, enabling an assessment of the modeling accuracy (see Table 6).

Beyond the studies already mentioned in Section 4.1, an interesting application domain is found in Concentrated Solar Power receivers. In [114], small stainless-steel samples equipped with Diamond-sheet and SplitP-sheet lattices are tested in a solar simulator. Both TPMS exhibit excellent heat removal capabilities, with the SplitP-sheet providing the best overall performance.

The concept of employing TPMS as a porous cooling medium is investigated experimentally in [51], focusing on transpiration cooling for gas-turbine hot-gas-path components. A Diamond-solid lattice is used as the porous insert, and the cooling film formed by coolant percolating through the structure provides effective thermal protection. For completeness, we note that Gyroid lattices have also been explored as porous cooling media in [50], where the cooling efficiency is shown to depend strongly on porosity at fixed blowing rate. A related configuration, named“effusion cooling”, is analyzed in [77], in [184] and in [185]. Numerical results indicate that Diamond-based TPMS yields a more uniform flow distribution and lower thermal stresses compared to pin-based solutions. Further optimization

of the same design, primarily by removing lattice material near the outlets, is presented in [185].

Other numerical studies aim at investigating the fundamental thermal-hydraulic behavior of Diamond lattices. In [42], seven Diamond-sheet cells are placed in a square channel heated on one side. The cell size is kept constant, whereas the porosity is varied by changing the wall thickness. The results show that the wall-thickness effect on heat transfer is negligible for $Re < 25$, but the associated decrease in porosity leads to a substantial reduction in PEC under laminar conditions. A larger computational domain, consisting of ten consecutive cells, is used in [171] to compare the thermal-hydraulic performance of several TPMS, including Diamond-solid, Gyroid-solid, Lidinoid-solid, Primitive-solid, and Neovius-solid. In this extensive comparison, the Diamond lattice consistently displays the best performance.

The combined experimental-numerical study [175] investigates Diamond-solid lattices subjected to controlled geometric stretching. By compressing or elongating the lattice in directions parallel or orthogonal to the flow, the authors identify deformation configurations capable of reducing the pressure drop while enhancing the overall PEC. A similar mixed approach is adopted in [176], which analyses Diamond-sheet and Diamond-solid lattices. The numerical simulations rely on a $1 \times 1 \times 5$-cell domain embedded in a one-sided-heated square channel under turbulent flow. The ranking based on PEC identifies the Diamond-sheet as the most efficient configuration. The study also highlights the importance of manufacturing tolerances, which significantly affect porosity and local wall thickness.

A further contribution is offered by [143], where a novel metric is introduced to quantify effective heat penetration into the fluid. The metric is defined as the ratio between the cross-sectional area having a dimensionless temperature greater than 1% of the reference wall temperature, and the total area. This indicator allows an alternative assessment of the effect of introducing Diamond-sheet TPMS into a heat sink, particularly relevant at high Biot numbers where convective transport dominates. However, the metric does not account for the pressure-drop penalty and therefore should be considered complementary to more conventional thermal-hydraulic figures of merit. The authors note that hybrid solutions, combining TPMS with more traditional cooling elements, may be advantageous at low Biot numbers.

Overall, the Diamond-based HS literature reveals a consistent pattern: Strong reliance on turbulent-air studies, frequent use of short lattice rows, significant sensitivity of the performance to porosity, and manufacturing deviations, and a variety of performance metrics that complicate cross-study comparisons. These recurring aspects will be reconsidered in the broader analysis of Section 5.

4.2. Studies on Heat Exchangers

A summary of the studies performed on heat exchangers equipped with TPMS is reported in Figure 14. The pie chart highlights that, although Gyroid and Diamond remain the most common choices, non-self-complementary topologies such as Neovius, SplitP, and I-WP have been explored for HX applications (although only in a limited number of studies). The accompanying sunburst plots further resolve, for Gyroid and Diamond lattices, the working fluids employed (DI7), the flow regimes (DI11), and the type of study (DI5).

Gyroids dominate the literature on TPMS-based HX (Table 7), followed by Diamond lattices (Table 8). Most studies investigate water-to-water configurations, often with one stream on each side of the TPMS core. A number of contributions also propose correlations for the Nusselt number or performance comparisons against conventional HX types.

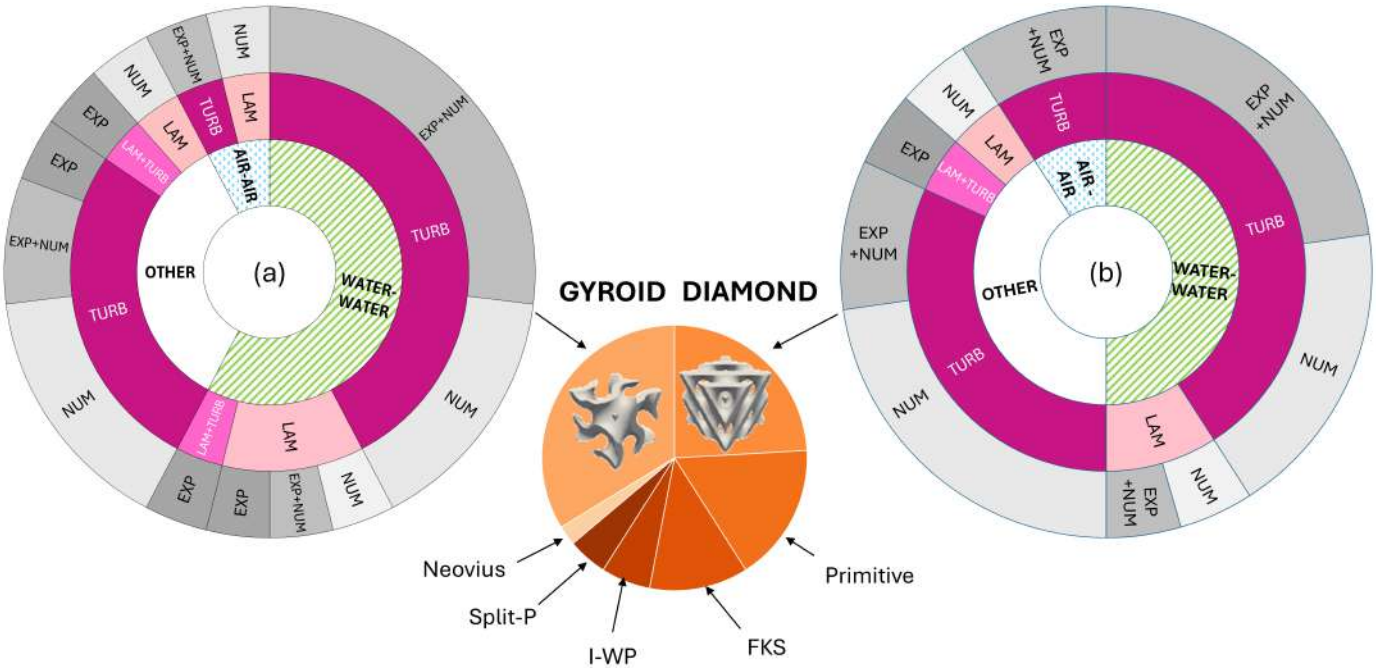

Figure 14. Distribution of the results for the Data Item DI10, for the papers relative to HX (Pie chart). The details on the flow regime (DI11) and type of study (DI5) for the different operating fluids (DI7) investigated in the studies involving G (**a**) and D (**b**) lattices are also reported.

Table 7. Publications on HX, involving Gyroid topology.

Ref	Fluids	Type of Study	Validation	Flow Regime	Turb. Model	Sim. Software
[130]	Air + Water	EXP	–	TURB + LAM	–	–
[107]	Air + Water	EXP, NUM	–	TURB	Realizable k-ε	ANSYS Fluent
[101]	Air + Air	EXP, NUM	X	TURB	k-ω SST	ANSYS CFX
[53]	Air + Air	NUM	–	LAM	–	COMSOL
[99]	CO_2 + CO_2	NUM	X	TURB	k-ω SST	ANSYS CFX
[135]	Oil + Water	NUM	X	LAM	–	COMSOL
[145]	Fuel + Oil	NUM	X	TURB	k-ω SST	–
[120]	R134-a + Glycol water	EXP	–	TURB	–	–
[49]	Water + Air + Acetone	NUM	X	TURB	k-ω SST	ANSYS Fluent
[98]	Water + SCO_2	NUM	–	TURB	k-ω SST	ANSYS CFX
[91]	Water + Water	EXP	–	LAM	–	–
[89]	Water + Water	EXP	–	LAM + TURB	–	–
[62]	Water + Water	EXP, NUM	X	LAM	–	COMSOL
[92]	Water + Water	EXP, NUM	–	TURB	k-ω SST	ANSYS Fluent
[119]	Water + Water	EXP, NUM	–	TURB	k-ω SST	ANSYS Fluent
[174]	Water + Water	EXP, NUM	–	TURB	k-ω SST	OpenFoam
[115]	Water + Water	EXP, NUM	–	TURB	Standard k-ε	Simerics-MP+
[103]	Water + Water	EXP, NUM	X	TURB	k-ω SST	ANSYS Fluent
[104]	Water + Water	EXP, NUM	X	TURB	k-ω	ANSYS Fluent
[178]	Water + Water	EXP, NUM	X	TURB	k-ω SST	OpenFoam
[82]	Water + Water	NUM	–	LAM	–	COMSOL
[35]	Water + Water	NUM	–	TURB	Realizable k-ε	STAR-CCM+
[108]	Water + Water	NUM	–	TURB	k-ω SST	ANSYS Fluent
[144]	Water + Water	NUM	–	TURB	k-ω SST	ANSYS Fluent
[179]	Water + Water	NUM	X	TURB	k-ω SST	OpenFoam
[168]	Water/Glycol + Water/Glycol	EXP, NUM	X	TURB	Standard k-ε	ANSYS Fluent
[83]	–	NUM	–	–	–	–

Table 8. Publications on HX, involving Diamond topology.

Ref	Fluids	Type of Study	Validation	Flow Regime	Turb. Model	Sim. Software
[101]	Air + Air	EXP, NUM	X	TURB	*k-ω* SST	ANSYSCFX
[102]	Air + Air	EXP, NUM	–	TURB	*k-ω* SST	ANSYSCFX
[130]	Air + Water	EXP	–	TURB + LAM	–	–
[99]	CO_2 + CO_2	NUM	X	TURB	*k-ω* SST	ANSYSCFX
[79]	He + H_2	NUM	X	TURB	*k-ω* SST	ANSYS Fluent
[135]	Oil + Water	NUM	X	LAM	–	COMSOL
[146]	Oil + Oil	NUM	X	TURB	*k-ω*	ANSYS Fluent
[49]	Water + Air + Acetone	NUM	X	TURB	*k-ω* SST	ANSYS Fluent
[98]	Water + SCO_2	NUM	–	TURB	*k-ω* SST	ANSYSCFX
[89]	Water + Water	EXP	–	LAM + TURB	–	–
[75]	Water + Water	EXP, NUM	–	LAM	–	ANSYS Fluent
[76]	Water + Water	EXP, NUM	–	TURB	*k-ω* SST	ANSYS Fluent
[119]	Water + Water	EXP, NUM	–	TURB	*k-ω* SST	ANSYS Fluent
[103]	Water + Water	EXP, NUM	X	TURB	*k-ω* SST	ANSYS Fluent
[104]	Water + Water	EXP, NUM	X	TURB	*k-ω*	ANSYS Fluent
[131]	Water + Water	EXP, NUM	X	TURB	Realizable *k-ε*	STAR-CCM+
[82]	Water + Water	NUM	–	LAM	–	COMSOL
[108]	Water + Water	NUM	–	TURB	*k-ω* SST	ANSYS Fluent
[144]	Water + Water	NUM	–	TURB	*k-ω* SST	ANSYS Fluent
[179]	Water + Water	NUM	X	TURB	*k-ω* SST	OpenFoam
[168]	Water/Glycol + Water/Glycol	EXP, NUM	X	TURB	Standard *k-ε*	ANSYS Fluent

The authors of [80] explicitly address the lack of detailed heat-transfer characterization in TPMS HX. Their work presents an experimental campaign on a counter-flow HX 3D-printed in AISI 316L. By combining measurements from both hot and cold sides, they derive a Nusselt-number correlation for single-phase water flow. A complementary configuration is studied in [62], where a cross-flow HX printed in resin enables wall thicknesses below 0.5 mm and laminar-flow testing. The Gyroid-based HX demonstrates higher efficiency at fixed NTU values than a broad set of compact and non-compact HX. A further Nu correlation is proposed in [178] for another Gyroid-based cross-flow HX, combining experiments and numerical simulations.

A purely numerical comparison of several TPMS (Gyroid, Diamond, Primitive, Neovius, FRD, and FKS) is conducted in [82]. Simulations are performed on a $1 \times 1 \times 4$ unit-cell domain, periodic in the transverse direction, and for different unit-cell sizes. In laminar flow, the Diamond-based HX achieves heat-transfer levels comparable to tubular HX while occupying an order-of-magnitude smaller volume, highlighting the compactness benefits of TPMS.

Most other water-water studies consider the entire HX component, rather than isolated cells. In [92], a counter-flow Gyroid HX is characterised numerically and experimentally. Among the tested RANS models, the *k-ω* SST closure shows the best agreement with experiments. The numerical analysis indicates that heat transfer scales approximately linearly with the inverse of the cell size, whereas the pressure drop increases more steeply. An evaluation of entropy generation is also provided, emphasizing the trade-off between compactness and pressure losses. The authors stress the relevance of customization and compactness when justifying the use of TPMS in HX.

In [53], a single Gyroid cell is investigated in counter-current air-air operation for $50 \leq \mathrm{Re} \leq 150$, primarily assessing the effect of wall thickness. The study [101] extends this approach by experimentally and numerically analysing three cross-flow metal HX using Primitive, Gyroid, and Diamond lattices. All prototypes exhibit good dimensional accuracy and structural integrity. The Diamond lattice provides the highest efficiency with

a lower pressure drop than the other topologies. Follow-up work by the same group, [50], investigates different Diamond cell sizes and confirms that HX effectiveness increases as cell size decreases.

Diamond-based HX are also confirmed to offer superior performance in [144]. The study includes optimizing the lattice regions near the manifolds to reduce pressure losses. Similarly, [131] compares Diamond-based HX to plate HX via simulations and tests, and investigates alternative manifold geometries, targeting pressure-drop reduction with minimal impact on heat transfer.

The numerical comparison of Gyroid, Diamond, and SplitP lattices in [103] shows that wall thickness, lattice unit length and material conductivity have a significant impact on heat transfer. The numerical results for Gyroid lattices exhibit excellent agreement with measurements from an aluminium HX. The achieved heat-transfer coefficient is much higher than that of a commercial compact HX of comparable power.

Ultra-compact Diamond HX are analyzed experimentally and numerically in [75,76]. The first work compares TPMS HXs manufactured from different materials against a plate HX, showing substantial gains in the volumetric heat-transfer coefficient for the TPMS designs. The numerical results confirm that Diamond lattices promote more uniform temperature and velocity fields. The second work examines different Diamond cell sizes and reports that the manufactured wall thicknesses (via SLM) exceed the design values by over 25%, which significantly affects both pressure drop and heat transfer. Note, however, that the numerical simulation of TPMS with rough surfaces remains a challenge.

Three additional studies provide combined numerical-experimental investigations of full HX prototypes: [104,115,174]. These works highlight the feasibility of lattice grading in practical HX design and the beneficial effect of abrasive-jet cleaning on pressure drop when metallic TPMS are used.

Several contributions focus on purely numerical analyses of cross-flow HX with different TPMS. In [35], the efficiency-NTU values of Gyroid- and Primitive-based HX are compared to theoretical cross-flow correlations. TPMS HX has been shown to achieve significantly higher efficiencies, and at a fixed NTU, the Primitive lattice outperforms the Gyroid. The general applicability of the effectiveness-NTU method to TPMS with complex internal flows is demonstrated in [102] for a Diamond-based air-to-air HX operating in a turbulent regime. The study [108] additionally considers hybrid Gyroid-Diamond configurations. Although Gyroid lattices yield the most favorable Nusselt-number distribution, some hybrid solutions show potential to surpass the baseline topologies.

Finally, Table 7 also includes the topology optimization analysis presented in [83], which relies on analytical shape functions rather than discretized flow equations. This work illustrates how the mathematical structure of TPMS can be used directly for optimization purposes, without requiring the full numerical resolution of the governing equations.

5. Discussion and Research Outlook

This work provides the first systematic, reproducible assessment of Triply Periodic Minimal Surfaces for thermal management, covering heat-transfer applications over a 25-year period and using the APISSER methodology to ensure transparency in paper identification, screening, and data extraction. The present study analyses a large body of literature, with sixty HS papers adopting Gyroid and Diamond lattices and almost forty HX studies. This extended coverage provides a more comprehensive perspective on the state of the art and enables trends that were previously difficult to discern in previous reviews. The certainty of the resulting highlights was qualitatively confirmed by agreement with conclusions reported in previous reviews.

The objective methodology used for paper identification identified "false negative" papers, excluded from the database mainly because they lacked evidence of the keywords used in the present analysis. This finding suggests greater care in the phrasing of the title and abstract for future papers on the topic.

An initial observation about the papers extracted from the database is the dominance of numerical studies. CFD is the primary modeling tool across all applications, and turbulent flows are almost always analyzed using RANS closures, especially the k-ω SST and Realizable k-ε models. While these models often provide reasonable global predictions, detailed validation remains limited. Experimental datasets are scarce and, when available, are generally used only for partial comparisons. Verification and validation practices, including uncertainty quantification and standardized procedures such as the ASME V&V one, are seldom adopted. In addition, most simulations employ short computational domains (typically four or five unit cells), resulting in limited control over entrance effects and the onset of fully developed flow, which directly affects the accuracy of derived Nusselt number and friction factor correlations. Moreover, given the geometric complexity of TPMS and the presence of strong mixing and curvature-driven flow structures, RANS closures may not always capture the relevant physics. Targeted LES or DNS studies on limited domains (one or two unit cells) could provide valuable reference data for model calibration. Similarly, there is a need for experimental campaigns providing spatially resolved heat-transfer and pressure fields to support reproducible validation.The limited and heterogeneous validation practices identified in Section 3.10, have also direct implications for the reliability of performance rankings and heat transfer correlations reported in the literature. In the absence of systematic quantitative validation, differences in predicted performance between TPMS topologies may reflect modeling assumptions rather than genuine physical superiority. This issue is particularly critical when PEC-based rankings are used to guide design decisions, as small discrepancies in pressure-drop or heat-transfer predictions can lead to markedly different conclusions.

The analysis also highlights a systematic separation in the way momentum and heat transfer are treated. Pressure-drop data, which are also the main topic of dedicated studies restricted to the hydraulic analysis, not directly addressed here, are often interpreted using porous-medium concepts, highlighting the transitions between viscous, inertial, and turbulent regimes. However, heat-transfer performance is evaluated using correlations of the form $\mathrm{Nu} = A\,\mathrm{Re}^{m}\mathrm{Pr}^{n}$, even though the underlying assumptions were not originally formulated for TPMS lattices. As a consequence, the coupling between momentum and energy transport remains insufficiently explored, and TPMS-specific correlations are still lacking.

Another important dimension emerging from this review concerns the role of geometry and manufacturability. Gyroid and Diamond lattices remain the most widely studied topologies, but cell size, wall thickness, porosity, and graded variations often play as significant a role as the topology itself. Moreover, deviations introduced by Additive Manufacturing, especially in SLM-produced lattices, modify the effective hydraulic diameter, porosity, and surface roughness, and this issue is addressed in only a limited number of studies. In TPMS lattices, additive manufacturing deviations cannot be regarded as minor geometric imperfections. Local wall-thickness variations and surface roughness act as distributed turbulators, altering near-wall flow physics and fundamentally affecting both pressure losses and convective heat transfer. As a consequence, discrepancies between smooth-wall CFD predictions and experimental measurements are systematic rather than incidental, and their impact increases with Reynolds number. To improve the comparability between numerical and experimental studies, the following minimum reporting checklist is recommended for TPMS thermo-hydraulic investigations:

- CAD porosity versus as-built porosity, explicitly reported and compared;

- Effective hydraulic diameter or permeability-based equivalent, derived from the as-built geometry;
- At least one areal surface roughness metric (e.g., arithmetic mean height or root mean square height of roughness);
- Explicit indication of whether the numerical model is based on ideal CAD geometry or reconstructed geometry (e.g., from micro-CT scans).

Without this information, comparisons between experiments and simulations remain intrinsically ambiguous, and discrepancies are often incorrectly attributed to turbulence modeling or numerical schemes. By contrast, explicitly accounting for manufacturing-induced geometric effects provides a physically grounded basis for validation and significantly improves the interpretability of thermohydraulic performance metrics.

On the other side, manufacturing artifacts are not merely geometric imperfections; they act as distributed turbulators that fundamentally alter near-wall flow physics. Consequently, experimental pressure drops are often systematically higher than those predicted by smooth-wall CFD, leading to discrepancies in the derived friction factors and Nusselt-number correlations. To bridge this prediction gap, future numerical research should move beyond idealized CAD geometries and adopt high-fidelity modeling strategies. Practical approaches include reconstructing computational domains directly from X-ray micro-CT scans of printed samples, thereby capturing as-built geometry and local wall-thickness variations, and incorporating calibrated roughness or distributed turbulator models into the boundary conditions. Wherever possible, numerical reconstructions should be validated against quantitative surface-characterization data, for example, areal roughness metrics, and spatially resolved experimental measurements of pressure and near-wall flow so that simulations are both physically realistic and quantitatively predictive.

A further challenge lies in comparing different TPMS configurations. A key conclusion of this systematic analysis is that the TPMS research community would greatly benefit from the establishment of a common standard for performance metrics and a shared set of reference benchmarks. Currently, inconsistencies in the definitions of non-dimensional groups and performance metrics hinder direct comparisons between studies. A recurring difficulty concerns the use of classical performance criteria, such as Webb's Performance Evaluation Criterion (PEC), which were not originally formulated for porous-like structures such as TPMS. Variations in the definition of pumping power, reference velocity, or hydraulic diameter lead to inconsistent rankings of Gyroid, Diamond, and other topologies. Alternative metrics, such as local temperature-based measures or heat penetration ratios, provide valuable insights but do not account for the hydraulic penalty of the lattice. The metric referring to the area goodness factor (i.e., the ratio between the Colburn and friction factors) accounts for the hydraulic penalty, but is adopted only in a limited number of studies. Developing a performance metric tailored to TPMS that reflects their geometric complexity and flow characteristics would greatly improve the comparability and interpretability of future results. To translate the above considerations into pragmatic guidelines, Table 9 proposes a minimum set of standardized definitions that should be explicitly reported in TPMS thermo-hydraulic studies to ensure comparability and reproducibility.

A key outcome of this work is the structured database (S-DB) provided as Supplementary Material. Beyond supporting the present analysis, the S-DB is intended as a reusable research tool that enables rapid identification of studies matching specific combinations of TPMS topology, application (HS, HX), working fluid, flow regime, modeling approach, and validation level. By making the underlying metadata explicitly accessible, the database facilitates benchmarking, model validation, and the design of future experimental and numerical investigations. The APISSER-based TPMS database developed in this work, for the first time, consolidates fragmented literature into a coherent picture and reveals recurring

research gaps. By covering a significantly broader set of studies than previous reviews, this work provides a robust foundation for benchmarking, topology selection, and the design of next-generation TPMS-based thermal systems. The database and methodology presented here offer a reproducible framework that can support future research directions and promote the development of more reliable, efficient, and validated TPMS thermal components. A limitation of the review process is the reliance on a single bibliographic database (Scopus), which may have led to the exclusion of relevant studies indexed elsewhere. Moreover, the classification of studies relies on information explicitly reported in the papers, which may introduce uncertainty when methodological details are incompletely described. As a final disclaimer, the review was not registered in any public database, no formal review protocol was prepared prior to conducting the study, and no formal assessment of reporting bias was conducted, as the review does not include quantitative effect synthesis.

Table 9. Recommended minimum definitions for thermo-hydraulic quantities used in TPMS performance evaluation.

Quantity	Recommended Definition	Comment
Reference velocity	Pore velocity (based on total cross-sectional area scaled by porosity)	Superficial velocity is insensitive to porosity
Reynolds number	Based on pore velocity	Accounts for porosity-dependent scaling
Hydraulic diameter	Porosity-based or permeability-based equivalent	Channel-based diameter is not meaningful in TPMS
Friction factor	Explicitly state the Darcy or Fanning formulation	Mixing the two alters PEC values
Pumping power	$\Delta p \cdot Q$ based on the same reference velocity	Prevents artificial efficiency gains or losses
Nusselt number	Based on a consistent reference temperature and hydraulic diameter	Avoid mixed or biased definitions

Supplementary Materials: The following supporting information can be downloaded at: https://www.mdpi.com/article/10.3390/en19030833/s1.

Author Contributions: Conceptualization, L.S. and L.M.; methodology, L.S. and L.M.; software, A.Q.T.; validation, A.Q.T. and W.F.; formal analysis, L.S., W.F. and L.M.; investigation, L.M.; resources, L.S.; data curation, A.Q.T., L.S. and W.F.; writing—original draft preparation, L.S., L.M. and W.F.; writing—review and editing, L.S., L.M., A.Q.T., A.C. and W.F.; visualization, L.S.; supervision, L.S.; project administration, L.S. and L.M. All authors have read and agreed to the published version of the manuscript.

Funding: This research has received no funding.

Data Availability Statement: The database (S-DB) presented in this study is included in the article/Supplementary Materials. Further inquiries can be directed to the corresponding author.

Acknowledgments: During the preparation of this manuscript, the authors used ChatGPT (version 5.1, OpenAI) for the purpose of revising the grammar and syntax of the text. The authors reviewed and edited the output and take full responsibility for the content of this publication.

Conflicts of Interest: The authors declare no conflicts of interest.

Abbreviations

The following abbreviations are used in this manuscript:

AM	Additive Manufacturing
BCC	Body-Centered Cubic
CFD	Computational Fluid Dynamics
CP	Cubic Primitive

D	Diamond
DLP	Digital Light Processing
DI	Data Item
DMLS	Direct Metal Laser Sintering
DNS	Direct Numerical Simulation
EXC	Exclusion Criterion
EXP	Experimental
FC	Free Convection
FDM	Fused Deposition Modeling
FKS	Fischer–Koch S
G	Gyroid
HS	Heat Sink
HX	Heat Exchanger
IN	Inclusion Criterion
LAM	Laminar
LCD	Liquid Crystal Display
LES	Large Eddy Simulation
L-PBF	Laser Powder Bed Fusion
NUM	Numerical
O-DB	Online DataBase
P	Primitive
PCM	Phase-Change Material
PEC	Performance Evaluation Criterion
PBF	Powder Bed Fusion
RANS	Reynolds-Averaged Navier–Stokes
RQ	Research Question
S-DB	Short DataBase
SLA	Stereolithography
SLM	Selective Laser Melting
SLS	Selective Laser Sintering
TP	Thermo-Physical Properties
TPMS	Triply Periodic Minimal Surfaces
TURB	Turbulent
VAL	Validation

References

1. Dutkowski, K.; Kruzel, M.; Rokosz, K. Review of the State-of-the-Art Uses of Minimal Surfaces in Heat Transfer. *Energies* **2022**, *15*, 7994. [CrossRef]
2. Yeranee, K.; Rao, Y. A Review of Recent Investigations on Flow and Heat Transfer Enhancement in Cooling Channels Embedded with Triply Periodic Minimal Surfaces (TPMS). *Energies* **2022**, *15*, 8994. [CrossRef]
3. Gado, M.G.; Al-Ketan, O.; Aziz, M.; Al-Rub, R.A.; Ookawara, S. Triply Periodic Minimal Surface Structures: Design, Fabrication, 3D Printing Techniques, State-of-the-Art Studies, and Prospective Thermal Applications for Efficient Energy Utilization. *Energy Technol.* **2024**, *12*, 2301287. [CrossRef]
4. Wang, H.; Zhao, C.; Liu, W.; Liu, Z.; Bian, H.; Zhang, K. Advances in triply periodic minimal surface structures for thermal management systems: A comprehensive review. *Appl. Therm. Eng.* **2025**, *279*, 127481. [CrossRef]
5. Castillo, S.; Grbovic, P. The APISSER Methodology for Systematic Literature Reviews in Engineering. *IEEE Access* **2022**, *10*, 23700–23707. [CrossRef]
6. Page, M.J.; McKenzie, J.E.; Bossuyt, P.M.; Boutron, I.; Hoffmann, T.C.; Mulrow, C.D.; Shamseer, L.; Tetzlaff, J.M.; Akl, E.A.; Brennan, S.E.; et al. The PRISMA 2020 statement: An updated guideline for reporting systematic reviews. *BMJ* **2021**, *372*, n71. [CrossRef]
7. Elsevier. Scopus; Elsevier: Amsterdam, The Netherlands, 2024. Available online: https://www.scopus.com (accessed on 16 October 2025).
8. Clarivate Analytics. Web of Science; Clarivate Analytics: Philadelphia, PA, USA, 2024. Available online: https://www.webofscience.com (accessed on 16 October 2025).

9. IEEE. IEEE Xplore Digital Library; Institute of Electrical and Electronics Engineers: Piscataway, NJ, USA, 2024. Available online: https://ieeexplore.ieee.org (accessed on 16 October 2025).
10. Luo, J.W.; Chen, L.; Min, T.; Shan, F.; Kang, Q.; Tao, W.Q. Macroscopic transport properties of Gyroid structures based on pore-scale studies: Permeability, diffusivity and thermal conductivity. *Int. J. Heat Mass Transf.* **2020**, *146*, 118837. [CrossRef]
11. Aider, Y.; Kaur, I.; Cho, H.; Singh, P. Periodic heat transfer characteristics of additively manufactured lattices. *Int. J. Heat Mass Transf.* **2022**, *189*, 122692. [CrossRef]
12. Bonner-Hutton, O.; Busch, B.; Lv, Y.; Caughley, A.; Badcock, R.; Lumsden, G.; Weijers, H.; Singamneni, S. Analysis of Gyroid Heat Exchangers for Superconducting Electric Motors. *Mater. Today Proc.* 2023, *in press*. [CrossRef]
13. Moradmand, M.; Sohankar, A. Numerical and experimental investigations on the thermal-hydraulic performance of heat exchangers with Schwarz-P and gyroid structures. *Int. J. Therm. Sci.* **2024**, *197*, 108748. [CrossRef]
14. Mahmoodi, M.; Sohankar, A.; Joulaei, A. Investigations of nanofluid flow and heat transfer in a rotating microchannel using single- and two-phase approaches. *Numer. Heat Transf. Part A Appl.* **2023**, *83*, 80–115. [CrossRef]
15. Ali, D.; Ozalp, M.; Blanquer, S.B.; Onel, S. Permeability and fluid flow-induced wall shear stress in bone scaffolds with TPMS and lattice architectures: A CFD analysis. *Eur. J. Mech.-B/Fluids* **2020**, *79*, 376–385. [CrossRef]
16. Bobbert, F.; Lietaert, K.; Eftekhari, A.; Pouran, B.; Ahmadi, S.; Weinans, H.; Zadpoor, A. Additively manufactured metallic porous biomaterials based on minimal surfaces: A unique combination of topological, mechanical, and mass transport properties. *Acta Biomater.* **2017**, *53*, 572–584. [CrossRef]
17. Bragin, D.; Karpilov, I.; Pashchenko, D. Flow dynamics through cellular material based on a structure with triply periodic minimal surface. *Chem. Eng. Sci.* **2024**, *298*, 120291. [CrossRef]
18. Chouhan, G.; Gunji, B. Additive manufacturing TPMS lattice structures: Experimental study on airflow resistivity. *Results Mater.* **2023**, *20*, 100478. [CrossRef]
19. Clarke, D.A.; Dolamore, F.; Fee, C.J.; Galvosas, P.; Holland, D.J. Investigation of flow through triply periodic minimal surface-structured porous media using MRI and CFD. *Chem. Eng. Sci.* **2021**, *231*, 116264. [CrossRef]
20. Guerreiro, R.; Pires, T.; Guedes, J.M.; Fernandes, P.R.; Castro, A.P.G. On the Tortuosity of TPMS Scaffolds for Tissue Engineering. *Symmetry* **2020**, *12*, 596. [CrossRef]
21. Guest, J.K.; Prévost, J.H. Design of maximum permeability material structures. *Comput. Methods Appl. Mech. Eng.* **2007**, *196*, 1006–1017. [CrossRef]
22. Hawken, M.; Reid, S.; Clarke, D.; Watson, M.; Fee, C.; Holland, D. Characterization of pressure drop through Schwarz-Diamond triply periodic minimal surface porous media. *Chem. Eng. Sci.* **2023**, *280*, 119039. [CrossRef]
23. Hirokawa, T.; Miyata, H. Experimental investigation on pressure drop characteristics of adiabatic two-phase flow in a Gyroid-structured channel. *Int. J. Multiph. Flow* **2024**, *181*, 104982. [CrossRef]
24. Italiano, C.; Marino, G.; Thomas, M.; Hary, B.; Nardone, S.; Richard, S.; Saker, A.; Tasso, D.; Meynet, N.; Olivier, P.; et al. Carbon-Free H_2 Production from Ammonia Decomposition over 3D-Printed Ni-Alloy Structures Activated with a Ru/Al_2O_3 Catalyst. *Processes* **2024**, *12*, 2663. [CrossRef]
25. Kumar, J.; Nirala, N.s.; Singh, N.K.; Gupta, N.; Dwivedi, Y.D.; Verma, R.; Rai, S.K.; Gupta, M. Design, development and fluidic behavior analysis of triply periodic minimal surface (TPMS) based scaffolds for bone-applications. *Int. J. Interact. Des. Manuf.* **2024**, *18*, 3077–3087. [CrossRef]
26. Vhora, K.; Thévenin, D.; Janiga, G.; Sundmacher, K. CFD Analysis of the Flow in Schwarz-D TPMS Structures for Engineering Applications. *Chem. Ing. Tech.* **2024**, *96*, 1683–1696. [CrossRef]
27. Zeng, C.; Wang, W. Modeling method for variable and isotropic permeability design of porous material based on TPMS lattices. *Tribol. Int.* **2022**, *176*, 107913. [CrossRef]
28. Zhang, K.; Hickey, J.P.; Vlasea, M. An Analysis Framework of Additively Manufactured Deterministic Porous Structures for Transpiration Cooling. *J. Mater. Eng. Perform.* **2023**, *32*, 9253–9262. [CrossRef]
29. Zimmer, A.; PachecoAraújo, J.D.; Andreassen, K.A.; Grande, C.A. Effect of Manufacturing Techniques in Pressure Drop on Triple Periodical Minimal Surface Packings. *Chem. Ing. Tech.* **2021**, *93*, 967–973. [CrossRef]
30. Abdelqader, O.; Abu Al-Rub, R.K.; Hassan Ali, M.I. Atmospheric air freshwater using TPMS compact heat exchangers. *Appl. Therm. Eng.* **2024**, *246*, 122979. [CrossRef]
31. Abueidda, D.W.; Abu Al-Rub, R.K.; Dalaq, A.S.; Lee, D.W.; Khan, K.A.; Jasiuk, I. Effective conductivities and elastic moduli of novel foams with triply periodic minimal surfaces. *Mech. Mater.* **2016**, *95*, 102–115. [CrossRef]
32. Addin Burhan Al-Omari, S.; Qasem, M.; Ahmed Qureshi, Z.; Elnajjar, E.; Al-Ketan, O.; Abu Al-Rub, R. Design and performance assessment of a triply-periodic-minimal-surface structures-enhanced gallium heat sink for high heat flux dissipation: A numerical study. *Appl. Therm. Eng.* **2024**, *257*, 124154. [CrossRef]
33. Ahmed Qureshi, Z.; Addin Burhan Al-Omari, S.; Elnajjar, E.; Al-Ketan, O.; Abu Al-Rub, R. Architected lattices embedded with phase change materials for thermal management of high-power electronics: A numerical study. *Appl. Therm. Eng.* **2023**, *219*, 119420. [CrossRef]

34. Al-Ketan, O.; Ali, M.; Khalil, M.; Rowshan, R.; Khan, K.A.; Abu Al-Rub, R.K. Forced Convection Computational Fluid Dynamics Analysis of Architected and Three-Dimensional Printable Heat Sinks Based on Triply Periodic Minimal Surfaces. *J. Therm. Sci. Eng. Appl.* **2020**, *13*, 021010. [CrossRef]
35. Alteneiji, M.; Ali, M.I.H.; Khan, K.A.; Al-Rub, R.K.A. Heat transfer effectiveness characteristics maps for additively manufactured TPMS compact heat exchangers. *Energy Storage Sav.* **2022**, *1*, 153–161. [CrossRef]
36. Ansari, D.; Duwig, C. A gyroid TPMS heat sink for electronic cooling. *Energy Convers. Manag.* **2024**, *319*, 118918. [CrossRef]
37. Anwajler, B. The Thermal Properties of a Prototype Insulation with a Gyroid Structure—Optimization of the Structure of a Cellular Composite Made Using SLS Printing Technology. *Materials* **2022**, *15*, 1352. [CrossRef] [PubMed]
38. Anwajler, B.; Szołomicki, J.; Noszczyk, P.; Baryś, M. The potential of 3D printing in thermal insulating composite materials-experimental determination of the impact of the geometry on thermal resistance. *Materials* **2024**, *17*, 1202. [CrossRef] [PubMed]
39. Ashraf, J.M.; Taher, S.E.; Lee, D.W.; Liao, K.; Abu Al-Rub, R.K. On the computational modeling, additive manufacturing, and testing of tube-networks TPMS-based graphene lattices and characterizing their multifunctional properties. *APL Mater.* **2022**, *10*, 121107. [CrossRef]
40. Asif, M.; Grande, C.A. TPMS Contactors Designed with Imprinted Porosity: Numerical Evaluation of Momentum and Energy Transport. *Ind. Eng. Chem. Res.* **2022**, *61*, 18556–18566. [CrossRef]
41. Attarzadeh, R.; Attarzadeh-Niaki, S.H.; Duwig, C. Multi-objective optimization of TPMS-based heat exchangers for low-temperature waste heat recovery. *Appl. Therm. Eng.* **2022**, *212*, 118448. [CrossRef]
42. Attarzadeh, R.; Rovira, M.; Duwig, C. Design analysis of the "Schwartz D" based heat exchanger: A numerical study. *Int. J. Heat Mass Transf.* **2021**, *177*, 121415. [CrossRef]
43. Baobaid, N.; Ali, M.I.; Khan, K.A.; Abu Al-Rub, R.K. Fluid flow and heat transfer of porous TPMS architected heat sinks in free convection environment. *Case Stud. Therm. Eng.* **2022**, *33*, 101944. [CrossRef]
44. Barakat, A.; Sun, B. Controlling TPMS lattice deformation for enhanced convective heat transfer: A comparative study of Diamond and Gyroid structures. *Int. Commun. Heat Mass Transf.* **2024**, *154*, 107443. [CrossRef]
45. Barakat, A.; Sun, B. Enhanced convective heat transfer in new triply periodic minimal surface structures: Numerical and experimental investigation. *Int. J. Heat Mass Transf.* **2024**, *227*, 125538. [CrossRef]
46. Beer, M.; Rybár, R. Numerical Study of Fluid Flow in a Gyroid-Shaped Heat Transfer Element. *Energies* **2024**, *17*, 2244. [CrossRef]
47. Beer, M.; Rybár, R. Optimization of Heat Exchanger Performance Using Modified Gyroid-Based TPMS Structures. *Processes* **2024**, *12*, 2943. [CrossRef]
48. Bragin, D.; Popov, A.; Eremin, A. The thermal conductivity properties of porous materials based on TPMS. *Int. J. Heat Mass Transf.* **2024**, *231*, 125863. [CrossRef]
49. Brambati, G.; Guilizzoni, M.; Foletti, S. Convective heat transfer correlations for Triply Periodic Minimal Surfaces based heat exchangers. *Appl. Therm. Eng.* **2024**, *242*, 122492. [CrossRef]
50. Brimacombe, B.J.; Scobie, J.A.; Flynn, J.M.; Sangan, C.M.; Pountney, O.J. Effect of Porosity and Injection Ratio on the Performance of Transpiration Cooling through Gyroids. *Int. J. Turbomach. Propuls. Power* **2023**, *8*, 50. [CrossRef]
51. Broumand, M.; Son, J.; Pyo, Y.; Yun, S.; Hong, Z. TPMS-based transpiration cooling for film cooling enhancement. *Int. J. Heat Mass Transf.* **2024**, *231*, 125824. [CrossRef]
52. Catchpole-Smith, S.; Sélo, R.; Davis, A.; Ashcroft, I.; Tuck, C.; Clare, A. Thermal conductivity of TPMS lattice structures manufactured via laser powder bed fusion. *Addit. Manuf.* **2019**, *30*, 100846. [CrossRef]
53. Chen, F.; Jiang, X.; Lu, C.; Wang, Y.; Wen, P.; Shen, Q. Heat transfer efficiency enhancement of gyroid heat exchanger based on multidimensional gradient structure design. *Int. Commun. Heat Mass Transf.* **2023**, *149*, 107127. [CrossRef]
54. Chen, M.; Shi, Y.; Yang, L.; Yan, C.; Song, B.; Liu, Y.; Dou, Z.; Chen, Y. Thermal performances of Gyroid-fin heat sink for power chips. *Case Stud. Therm. Eng.* **2024**, *61*, 105095. [CrossRef]
55. Chen, W.; Tang, X.; Chu, X.; Yang, Y.; Xu, W.; Fu, D.; Li, X.; Zhou, W. Impact of catalyst carrier with TPMS structures on hydrogen production by methanol reforming. *Int. J. Hydrogen Energy* **2024**, *58*, 1177–1189. [CrossRef]
56. Cheng, Z.; Xu, R.; Jiang, P. Transpiration cooling with phase change by functionally graded porous media. *Int. J. Heat Mass Transf.* **2023**, *205*, 123862. [CrossRef]
57. Cheng, Z.; Li, S.; Chen, W.; Wang, Q. Modulation of Heat Transfer in a Porous Burner Based on Triply Periodic Minimal Surface. *ASME J. Heat Mass Transf.* **2023**, *145*, 052004. [CrossRef]
58. Cheng, Z.; Li, X.; Xu, R.; Jiang, P. Investigations on porous media customized by triply periodic minimal surface: Heat transfer correlations and strength performance. *Int. Commun. Heat Mass Transf.* **2021**, *129*, 105713. [CrossRef]
59. Cheng, Z.; Xu, R.; Jiang, P.X. Morphology, flow and heat transfer in triply periodic minimal surface based porous structures. *Int. J. Heat Mass Transf.* **2021**, *170*, 120902. [CrossRef]
60. Chi, Z.P.; Yang, G.H.; Wang, Q.H. Multi-morphological design of TPMS-based microchannels for thermal performance optimization. *Appl. Therm. Eng.* **2024**, *255*, 124050. [CrossRef]

61. Daifalla, E.; Shahpar, S.; Tristanto, I.; Carta, M. Multidisciplinary Optimization of Gyroid Topologies for a Cold Plate Heat Exchanger Design. *J. Eng. Gas Turbines Power* **2024**, *146*, 121028. [CrossRef]
62. Dixit, T.; Al-Hajri, E.; Paul, M.C.; Nithiarasu, P.; Kumar, S. High performance, microarchitected, compact heat exchanger enabled by 3D printing. *Appl. Therm. Eng.* **2022**, *210*, 118339. [CrossRef]
63. Dreißigacker, V.; Gutierrez, A. Latent Thermal Energy Storage for Cooling Demands in Battery Electric Vehicles: Development of a Dimensionless Model for the Identification of Effective Heat-Transferring Structures. *Energies* **2024**, *17*, 6218. [CrossRef]
64. Du, X.; Wang, Z.; Gao, Q.; Yang, H.; Bao, R.; Xiong, S. Study on novel battery thermal management using triply periodic minimal surface porous structures liquid cooling channel. *Appl. Therm. Eng.* **2024**, *257*, 124384. [CrossRef]
65. Dube Kerme, E.; Hajialibabei, M.; Ziad Saghir, M.; El-Ketan, O. Experimental investigation of porous gyroid structure: Effect of cell size and porosity on performance. *Therm. Sci. Eng. Prog.* **2024**, *53*, 102728. [CrossRef]
66. El Khadiri, I.; Abouelmajd, M.; Zemzami, M.; Hmina, N.; Lagache, M.; Belhouideg, S. Comprehensive analysis of flow and heat transfer performance in triply periodic minimal surface (TPMS) heat exchangers based on Fischer-Koch S, PMY, FRD, and Gyroid structures. *Int. Commun. Heat Mass Transf.* **2024**, *156*, 107617. [CrossRef]
67. Fan, Z.; Fu, Y.; Gao, R.; Liu, S. Investigation on heat transfer enhancement of phase change material for battery thermal energy storage system based on composite triply periodic minimal surface. *J. Energy Storage* **2023**, *57*, 106222. [CrossRef]
68. Fan, Z.; Gao, R.; Liu, S. Thermal conductivity enhancement and thermal saturation elimination designs of battery thermal management system for phase change materials based on triply periodic minimal surface. *Energy* **2022**, *259*, 125091. [CrossRef]
69. Fan, Z.; Gao, R.; Liu, S. A novel battery thermal management system based on P type triply periodic minimal surface. *Int. J. Heat Mass Transf.* **2022**, *194*, 123090. [CrossRef]
70. Fok, P.J.Y.; Kandasamy, R.; Ho, J.Y.; Wong, T.N. Enhancing the performance of composite phase change materials using novel triply periodic minimal surface structures. *Chem. Eng. J.* **2023**, *476*, 146352. [CrossRef]
71. Gado, M.G. Improving the charging performance of latent heat thermal energy storage systems using triply periodic minimal surface (TPMS) structures. *J. Energy Storage* **2024**, *103*, 114310. [CrossRef]
72. Gado, M.G.; Ookawara, S.; Hassan, H. Utilization of triply periodic minimal surfaces for performance enhancement of adsorption cooling systems: Computational fluid dynamics analysis. *Energy Convers. Manag.* **2023**, *277*, 116657. [CrossRef]
73. Gado, M.G.; Ookawara, S.; Nada, S.; Elkady, M.F.; Hassan, H. Adsorbent beds packed in triply periodic minimal surface-derived structures and their performance in adsorption desalination/cooling systems. *Int. Commun. Heat Mass Transf.* **2024**, *150*, 107205. [CrossRef]
74. Gajetti, E.; Bonesso, M.; Bruschi, A.; Fanale, F.; Garavaglia, S.; Granucci, G.; Moro, A.; Pepato, A.; Romano, A.; Savoldi, L. A New Efficient Mirror Cooling for the Transmission Line of Fusion Reactor ECH Systems Based on Triply Periodic Minimal Surfaces. *IEEE Trans. Plasma Sci.* **2024**, *52*, 3765–3771. [CrossRef]
75. Gao, S.; Ding, J.; Qu, S.; Liu, H.; Song, X. Numerical and experimental investigation of additively manufactured shell-lattice copper heat exchanger. *Int. Commun. Heat Mass Transf.* **2023**, *147*, 106976. [CrossRef]
76. Gao, S.; Qu, S.; Ding, J.; Liu, H.; Song, X. Influence of cell size and its gradient on thermo-hydraulic characteristics of triply periodic minimal surface heat exchangers. *Appl. Therm. Eng.* **2023**, *232*, 121098. [CrossRef]
77. Gu, H.; Liang, D.; Duan, P.; Zhou, D.; Li, W. Aerothermal characteristics of thin double-wall effusion cooling systems with novel slot holes and cellular architectures for gas turbines. *Aerosp. Sci. Technol.* **2023**, *140*, 108441. [CrossRef]
78. Huang, M.; Sha, W.; Xiao, M.; Gao, L.; Liu, X.; Wang, Y. Multiscale topology optimization of cellular structures with high thermal conductivity and large convective surface area. *Int. J. Therm. Sci.* **2024**, *201*, 109053. [CrossRef]
79. Huang, W.; Ning, H.; Li, N.; Tang, G.; Ma, Y.; Li, Z.; Nan, X.; Li, X. Thermal-hydraulic performance of TPMS-based regenerators in combined cycle aero-engine. *Appl. Therm. Eng.* **2024**, *250*, 123510. [CrossRef]
80. Ibhadode, O. The effects of cell stretching on the thermal and flow characteristics of triply periodic minimal surfaces. *Int. Commun. Heat Mass Transf.* **2024**, *153*, 107364. [CrossRef]
81. Iwaniszyn, M.; Sindera, K.; Maszybrocka, J.; Jodłowski, P.J. 3D-printed triply periodic minimal surface (TPMS) structures as catalyst carriers. *Chem. Eng. Res. Des.* **2024**, *209*, 37–51. [CrossRef]
82. Iyer, J.; Moore, T.; Nguyen, D.; Roy, P.; Stolaroff, J. Heat transfer and pressure drop characteristics of heat exchangers based on triply periodic minimal and periodic nodal surfaces. *Appl. Therm. Eng.* **2022**, *209*, 118192. [CrossRef]
83. Jiang, Y.; Hu, J.; Wang, S.; Lei, N.; Luo, Z.; Liu, L. Meshless Optimization of Triply Periodic Minimal Surface Based Two-Fluid Heat Exchanger. *Comput.-Aided Des.* **2023**, *162*, 103554. [CrossRef]
84. Jiang, X.; Lu, C.; Wen, P.; Chen, F. Synergetic enhancement of hydrogen concentration and heat transfer for triply periodic minimal surface based hydrogen storage reactor. *Int. J. Heat Mass Transf.* **2024**, *232*, 125965. [CrossRef]
85. Jivrakh, K.B.; Varghese, A.M.; Ehrling, S.; Kuppireddy, S.; Polychronopoulou, K.; Abu Al-Rub, R.K.; Alamoodi, N.; Karanikolos, G.N. 3D-printed zeolite 13X gyroid monolith adsorbents for CO_2 capture. *Chem. Eng. J.* **2024**, *497*, 154674. [CrossRef]
86. Jung, G.S.; Yeo, J.; Tian, Z.; Qin, Z.; Buehler, M.J. Unusually low and density-insensitive thermal conductivity of three-dimensional gyroid graphene. *Nanoscale* **2017**, *9*, 13477–13484. [CrossRef]

87. Kaur, I.; Singh, P. Flow and thermal transport characteristics of Triply-Periodic Minimal Surface (TPMS)-based gyroid and Schwarz-P cellular materials. *Numer. Heat Transf. A* **2021**, *79*, 553–569. [CrossRef]
88. Khalil, M.; Hassan Ali, M.I.; Khan, K.A.; Abu Al-Rub, R. Forced convection heat transfer in heat sinks with topologies based on triply periodic minimal surfaces. *Case Stud. Therm. Eng.* **2022**, *38*, 102313. [CrossRef]
89. Kim, J.; Yoo, D.J. 3D printed compact heat exchangers with mathematically defined core structures. *J. Comput. Des. Eng.* **2020**, *7*, 527–550. [CrossRef]
90. Knödler, P.; Dreissigacker, V. Fluid Dynamic Assessment and Development of Nusselt Correlations for Fischer Koch S Structures. *Energies* **2024**, *17*, 688. [CrossRef]
91. Kruzel, M.; Dutkowski, K.; Bohdal, T.; Litwin, A.; Sawicki, J.; Kepa, E. A new approach for heat transfer coefficient determination in triply periodic minimal surface-based heat exchangers. *Int. Commun. Heat Mass Transf.* **2024**, *157*, 107778. [CrossRef]
92. Kus, K.; Wójcik, M.; Malecha, Z.; Rogala, Z. Numerical and experimental investigation of the gyroid heat exchanger. *Int. J. Heat Mass Transf.* **2024**, *231*, 125882. [CrossRef]
93. Kwasi-Effah, C.C.; Ibhadode, O.; Qureshi, A. Thermo-hydraulic performance characteristics of novel G-Prime and FRD Triply Periodic Minimal Surface (TPMS) geometries. *Int. Commun. Heat Mass Transf.* **2024**, *159*, 108226. [CrossRef]
94. Lamotte-Dawaghreh, J.; Herring, J.; Pundla, S.A.; Suthar, R.; Nair, V.; Bansode, P.; Gupta, G.; Agonafer, D.; Madril, J.; Ouradnik, T.; et al. Electrochemical Additive Manufacturing-Based Design of a Heat Sink for Single-Phase Natural Convection Immersion Cooling Application. *J. Electron. Packag.* **2024**, *146*, 041113. [CrossRef]
95. Adhy Lesmana, L.; Lu, C.; Chen, F.; Aziz, M. Topology optimization of gyroid structure-based metal hydride reactor for high-performance hydrogen storage. *Therm. Sci. Eng. Prog.* **2024**, *50*, 102533. [CrossRef]
96. Lesmana, L.A.; Lu, C.; Chen, F.; Aziz, M. Triply periodic minimal surface gyroid structure as effective metal hydride hydrogen storage reactor: Experimental study. *Therm. Sci. Eng. Prog.* **2023**, *42*, 101903. [CrossRef]
97. Lesmana, L.A.; Aziz, M. Adoption of triply periodic minimal surface structure for effective metal hydride-based hydrogen storage. *Energy* **2023**, *262*, 125399. [CrossRef]
98. Li, W.; Li, W.; Yu, Z. Heat transfer enhancement of water-cooled triply periodic minimal surface heat exchangers. *Appl. Therm. Eng.* **2022**, *217*, 119198. [CrossRef]
99. Li, W.; Yu, G.; Yu, Z. Bioinspired heat exchangers based on triply periodic minimal surfaces for supercritical CO_2 cycles. *Appl. Therm. Eng.* **2020**, *179*, 115686. [CrossRef]
100. Li, W.; Ding, J.; Chen, X.; Wang, Y.; Song, X.; Zhang, S. 3D-printed CuNi alloy catalyst with triply periodic minimal surface for reverse water-gas shift reaction. *J. Mater. Chem. A Mater. Energy Sustain.* **2023**, *12*, 314–320. [CrossRef]
101. Liang, D.; Shi, C.; Li, W.; Chen, W.; Chyu, M.K. Design, flow characteristics and performance evaluation of bioinspired heat exchangers based on triply periodic minimal surfaces. *Int. J. Heat Mass Transf.* **2023**, *201*, 123620. [CrossRef]
102. Liang, D.; Yang, K.; Gu, H.; Chen, W.; Chyu, M.K. The effect of unit size on the flow and heat transfer performance of the "Schwartz-D" heat exchanger. *Int. J. Heat Mass Transf.* **2023**, *214*, 124367. [CrossRef]
103. Liu, J.; Cheng, D.; Oo, K.; McCrimmon, T.L.; Bai, S. Design and Additive Manufacturing of TPMS Heat Exchangers. *Appl. Sci.* **2024**, *14*, 3970. [CrossRef]
104. Liu, J.; Cheng, D.; Oo, K.; Pan, W.; McCrimmon, T.L.; Bai, S. Optimization of Triply Periodic Minimal Surface Heat Exchanger to Achieve Compactness, High Efficiency, and Low-Pressure Drop. *Energies* **2024**, *17*, 5141. [CrossRef]
105. Lu, R.; Zhang, Y.; Shen, M.; Yu, S.; Zhu, Y.; Xu, Y.; Liu, H.; Fu, R. 3D printing of a SiO_2@BN TPMS structure: Efficient heat transfer strategy for BN/epoxy composites. *Ceram. Int.* **2024**, *50*, 3820–3828. [CrossRef]
106. Ly, D.V.; Kishi, Y.; Nakayama, T.; Yamada, N. Thermal performance of polymer gyroid heat exchangers combined with phase change materials as a latent heat thermal energy storage system: An experimental investigation. *Int. J. Heat Mass Transf.* **2024**, *226*, 125531. [CrossRef]
107. Mahmoud, D.; Tandel, S.R.S.; Yakout, M.; Elbestawi, M.; Mattiello, F.; Paradiso, S.; Ching, C.; Zaher, M.; Abdelnabi, M. Enhancement of heat exchanger performance using additive manufacturing of gyroid lattice structures. *Int. J. Adv. Manuf. Technol.* **2023**, *126*, 4021–4036. [CrossRef]
108. Min, R.; Wang, Z.; Yang, H.; Bao, R.; Zhang, N. Heat transfer characterization of waste heat recovery heat exchanger based on flexible hybrid triply periodic minimal surfaces (TPMS). *Int. Commun. Heat Mass Transf.* **2024**, *157*, 107760. [CrossRef]
109. Mirabolghasemi, A.; Akbarzadeh, A.H.; Rodrigue, D.; Therriault, D. Thermal conductivity of architected cellular metamaterials. *Acta Mater.* **2019**, *174*, 61–80. [CrossRef]
110. Modrek, M.; Khan, K.A.; Ali, M.I.; Abu Al-Rub, R.K. Multi-objective topology optimization and numerical investigation of heat sinks based on triply periodic minimal surface lattices. *Case Stud. Therm. Eng.* **2024**, *63*, 105255. [CrossRef]
111. Modrek, M.; Viswanath, A.; Khan, K.A.; Ali, M.I.; Abu Al-Rub, R.K. An optimization case study to design additively manufacturable porous heat sinks based on triply periodic minimal surface (TPMS) lattices. *Case Stud. Therm. Eng.* **2022**, *36*, 102161. [CrossRef]

112. Modrek, M.; Viswanath, A.; Khan, K.A.; Hassan Ali, M.I.; Abu Al-Rub, R.K. Multi-objective topology optimization of passive heat sinks including self-weight based on triply periodic minimal surface lattices. *Case Stud. Therm. Eng.* **2023**, *42*, 102684. [CrossRef]
113. Molteni, M.; Candidori, S.; Graziosi, S.; Gariboldi, E. Improving the thermal response flexibility of 2- and 3-phase composite phase change materials by metallic triply periodic minimal surface structures. *J. Energy Storage* **2023**, *72*, 108185. [CrossRef]
114. Mortazavi, A.; Ávila Marín, A.; Ebadi, H.; Gajetti, E.; Piatti, C.; Marocco, L.; Savoldi, L. Experimental investigation of Triply Periodic Minimal Surfaces for high-temperature solar receivers. *Case Stud. Therm. Eng.* **2024**, *60*, 104771. [CrossRef]
115. Oh, S.H.; An, C.H.; Seo, B.; Kim, J.; Park, C.Y.; Park, K. Functional morphology change of TPMS structures for design and additive manufacturing of compact heat exchangers. *Addit. Manuf.* **2023**, *76*, 103778. [CrossRef]
116. Pelanconi, M.; Blyweert, P.; Bianchi, G.; Nicolas, V.; Viganò, D.; Bottacin, S.; Fierro, V.; Celzard, A.; Ortona, A. New, 3D binder-jetted carbons with minimal periodic surface structures. *Carbon* **2023**, *213*, 118252. [CrossRef]
117. Peng, C.; Long, R.; Liu, Z.; Liu, W. Improving adsorption hydrogen storage performance via triply periodic minimal surface structures with uniform and gradient porosities. *Int. J. Hydrogen Energy* **2024**, *53*, 422–433. [CrossRef]
118. Prussack, B.; Jentz, I.; Moreira, T.A.; Woolstenhulme, N.; Jesse, C.; Nellis, G.; Anderson, M. Thermal and hydraulic performance of volumetrically heated triply periodic minimal surface heaters. *Appl. Therm. Eng.* **2024**, *248*, 123291. [CrossRef]
119. Qian, C.; Wang, J.; Qiu, X.; Yan, L.; Yu, B.; Shi, J.; Chen, J. Numerical and experimental investigation of ultra-compact triply periodic minimal surface heat exchangers with high efficiency. *Int. J. Heat Mass Transf.* **2024**, *233*, 125984. [CrossRef]
120. Qian, C.; Wang, J.; Zhong, H.; Qiu, X.; Yu, B.; Shi, J.; Chen, J. Experimental investigation on heat transfer characteristics of copper heat exchangers based on triply periodic minimal surfaces (TPMS). *Int. Commun. Heat Mass Transf.* **2024**, *152*, 107292. [CrossRef]
121. Quamori Tanzi, A.; Cammi, A.; Marocco, L.; Savoldi, L. Design of a 10 MW/m^2-heat-flux removal system for a W7-X divertor tile using triply periodic minimal surfaces. *Case Stud. Therm. Eng.* **2024**, *63*, 105405. [CrossRef]
122. Qureshi, Z.A.; Addin Burhan Al-Omari, S.; Elnajjar, E.; Al-Ketan, O.; Al-Rub, R.A. On the effect of porosity and functional grading of 3D printable triply periodic minimal surface (TPMS) based architected lattices embedded with a phase change material. *Int. J. Heat Mass Transf.* **2022**, *183*, 122111. [CrossRef]
123. Qureshi, Z.A.; Al Omari, S.A.B.; Elnajjar, E.; Mahmoud, F.; Al-Ketan, O.; Al-Rub, R.A. Thermal characterization of 3D-Printed lattices based on triply periodic minimal surfaces embedded with organic phase change material. *Case Stud. Therm. Eng.* **2021**, *27*, 101315. [CrossRef]
124. Qureshi, Z.A.; Al-Omari, S.A.B.; Elnajjar, E.; Al-Ketan, O.; Abu Al-Rub, R. Nature-inspired triply periodic minimal surface-based structures in sheet and solid configurations for performance enhancement of a low-thermal-conductivity phase-change material for latent-heat thermal-energy-storage applications. *Int. J. Therm. Sci.* **2022**, *173*, 107361. [CrossRef]
125. Qureshi, Z.A.; Al-Omari, S.A.B.; Elnajjar, E.; Al-Ketan, O.; Al-Rub, R.A. Using triply periodic minimal surfaces (TPMS)-based metal foams structures as skeleton for metal-foam-PCM composites for thermal energy storage and energy management applications. *Int. Commun. Heat Mass Transf.* **2021**, *124*, 105265. [CrossRef]
126. Qureshi, Z.A.; Elnajjar, E.; Al-Ketan, O.; Al-Rub, R.A.; Al-Omari, S.B. Heat transfer performance of a finned metal foam-phase change material (FMF-PCM) system incorporating triply periodic minimal surfaces (TPMS). *Int. J. Heat Mass Transf.* **2021**, *170*, 121001. [CrossRef]
127. Rathore, S.S.; Mehta, B.; Kumar, P.; Asfer, M. Flow characterization in triply-periodic-minimal-surface (TPMS)-based porous geometries: Part 2—Heat transfer. *Transp. Porous Media* **2024**, *151*, 141–169. [CrossRef]
128. Rathore, S.S.; Mehta, B.; Kumar, P.; Asfer, M. Thermo-hydrodynamic performance evaluation of a mini-channel inserted with TPMS-based porous lattice. *J. Therm. Sci. Eng. Appl.* **2024**, *16*, 061009. [CrossRef]
129. Reid, S.; Symons, D.; Watson, M. Transient, multiscale, heterogeneous model of hydrogen peroxide decomposition for 3D-printed catalysts. *J. Propuls. Power* **2023**, *39*, 84–96. [CrossRef]
130. Reynolds, B.W.; Fee, C.J.; Morison, K.R.; Holland, D.J. Characterization of Heat Transfer within 3D Printed TPMS Heat Exchangers. *Int. J. Heat Mass Transf.* **2023**, *212*, 124264. [CrossRef]
131. Röver, T.; Kuehne, M.; Bischop, F.; Clague, L.; Bossen, B.; Emmelmann, C. Design and numerical assessment of an additively manufactured Schwarz diamond triply periodic minimal surface fluid-fluid heat exchanger. *J. Laser Appl.* **2023**, *35*, 042071. [CrossRef]
132. Sadeghi, F.; Baniassadi, M.; Shahidi, A.; Baghani, M. TPMS metamaterial structures based on shape memory polymers: Mechanical, thermal and thermomechanical assessment. *J. Mater. Res. Technol.* **2023**, *23*, 3726–3743. [CrossRef]
133. Saghir, M.Z.; Kerme, E.D.; Hajialibabei, M.; Rasheed, H.; Welsford, C.; Al-Ketan, O. Study of the Thermal and Hydraulic Performance of Porous Block versus Gyroid Structure: Experimental and Numerical Approaches. *Energies* **2024**, *17*, 861. [CrossRef]
134. Saghir, M.Z.; Rahman, M.M. Effectiveness in Cooling a Heat Sink in the Presence of a TPMS Porous Structure Comparing Two Different Flow Directions. *Fluids* **2024**, *9*, 297. [CrossRef]
135. Saghir, M.Z.; Yahya, M. Convection Heat Transfer and Performance Analysis of a Triply Periodic Minimal Surface (TPMS) for a Novel Heat Exchanger. *Energies* **2024**, *17*, 4275. [CrossRef]

136. Saghir, M.Z.; Kilic, G.A. Experimental forced convection study using a triply periodic minimal surface porous structure with a nanofluid: Comparison with numerical modeling. *Appl. Sci.* **2024**, *14*, 7594. [CrossRef]
137. Saghir, M.Z.; So, J.; Rasheed, H.; Ilesaliev, D. Forced Convection in Porous Medium Using Triply Periodical Minimum Surfaces. *Fluids* **2023**, *8*, 311. [CrossRef]
138. Saghir, M.Z.; Yahya, M. Cooling lithium-ion batteries in the presence of triply periodic minimal surfaces structure. *Appl. Sol. Energy* **2024**, *60*, 357–369. [CrossRef]
139. Salmon, F.; Lacanette, D.; Duquesne, M.; Godin, A. 3D fluid–structure simulation of innovative composites for the design and thermal management of electronic devices. *Energy Convers. Manag.* **2023**, *280*, 116824. [CrossRef]
140. Samson, S.; Tran, P.; Marzocca, P. Design and modeling of porous gyroid heatsinks: Influences of cell size, porosity and material variation. *Appl. Therm. Eng.* **2023**, *235*, 121296. [CrossRef]
141. Sauermoser-Yri, M.; Veldurthi, N.; Wölfle, C.H.; Svartvatn, P.J.; Flo Hoem, S.O.; Lid, M.J.; Bock, R.; Palko, J.W.; Torgersen, J. On the porosity-dependent permeability and conductivity of triply periodic minimal surface based porous media. *J. Mater. Res. Technol.* **2023**, *27*, 585–599. [CrossRef]
142. Seetoh, I.P.; Jovin, D.; Lai, C.Q. Effect of geometrical design on the latent heat cooling properties of a lightweight two-phase composite. *Appl. Phys. Lett.* **2021**, *119*, 141908. [CrossRef]
143. Shen, J.; Zhang, Q.; Wang, Z. Conjugate study on heat transfer enhancement of a TPMS-based hybrid heat sink design. *Appl. Therm. Eng.* **2024**, *257*, 124350. [CrossRef]
144. Shim, J.; Doh, J.; Park, S.i. Design framework based on implicit modeling for a compact heat exchanger with triply periodic minimal surface structures. *J. Mech. Sci. Technol.* **2024**, *38*, 4485–4496. [CrossRef]
145. Song, N.; Pu, W.; Qiao, L.; Wu, B.; Liu, R.; Luo, F. Numerical simulation study on the heat transfer and flow characteristics of fuel/lubricating oil heat exchanger based on triply periodic minimal surface (TPMS). *Appl. Therm. Eng.* **2024**, *257*, 124437. [CrossRef]
146. Song, Y.; Sun, Y.; Zou, Z.; Li, M.; Chen, W.; Du, F.; Zheng, W.; Hao, M. Systematic study of the thermal and hydraulic characteristics of a heat exchanger based on the Schwartz-D structure for aviation application. *Int. Commun. Heat Mass Transf.* **2024**, *156*, 107611. [CrossRef]
147. Stallard, S.; Jiang, H.; Chen, Y.; Bergman, T.L.; Li, X. Exploring the design space of the effective thermal conductivity, permeability, and stiffness of high-porosity foams. *Mater. Des.* **2023**, *231*, 112027. [CrossRef]
148. Sui, L.; Chen, B.; Liu, F.; Zhu, P.; Wang, H. Three-dimensional numerical simulation of solid-liquid phase change in the cavity of composite structures based on TPMS. *Appl. Therm. Eng.* **2024**, *238*, 122156. [CrossRef]
149. Tang, D.; Gao, T.; Chen, H.; Tian, M.; He, M.; Xu, S. Structure optimization and heat dissipation performance of additive-manufactured diamond/SiC and carbon fiber/SiC TPMS structural panel. *J. Manuf. Processes* **2024**, *127*, 589–598. [CrossRef]
150. Tang, D.; Xu, S.; Yang, K.; Gao, T.; Tang, H. Effects of porosity on effective thermal conductivities of thermal insulation SiC sandwich panels with Schoen-gyroid structure. *Ceram. Int.* **2024**, *50*, 10618–10625. [CrossRef]
151. Tang, W.; Guo, J.; Yang, F.; Zeng, L.; Wang, X.; Liu, W.; Zhang, J.; Zou, C.; Sun, L.; Zeng, Y.; et al. Performance analysis and optimization of the Gyroid-type triply periodic minimal surface heat sink incorporated with fin structures. *Appl. Therm. Eng.* **2024**, *255*, 123950. [CrossRef]
152. Tang, W.; Zhou, H.; Zeng, Y.; Yan, M.; Jiang, C.; Yang, P.; Li, Q.; Li, Z.; Fu, J.; Huang, Y.; et al. Analysis on the convective heat transfer process and performance evaluation of Triply Periodic Minimal Surface (TPMS) based on Diamond, Gyroid and Iwp. *Int. J. Heat Mass Transf.* **2023**, *201*, 123642. [CrossRef]
153. Tang, W.; Zou, C.; Zhou, H.; Zhang, L.; Zeng, Y.; Sun, L.; Zhao, Y.; Yan, M.; Fu, J.; Hu, J.; et al. A novel convective heat transfer enhancement method based on precise control of Gyroid-type TPMS lattice structure. *Appl. Therm. Eng.* **2023**, *230*, 120797. [CrossRef]
154. Thomas, N.; Sreedhar, N.; Al-Ketan, O.; Rowshan, R.; Abu Al-Rub, R.K.; Arafat, H. 3D printed triply periodic minimal surfaces as spacers for enhanced heat and mass transfer in membrane distillation. *Desalination* **2018**, *443*, 256–271. [CrossRef]
155. Thomas, N.; Swaminathan, J.; Zaragoza, G.; Abu Al-Rub, R.K.; Lienhard V, J.H.; Arafat, H.A. Comparative assessment of the effects of 3D printed feed spacers on process performance in MD systems. *Desalination* **2021**, *503*, 114940. [CrossRef]
156. Tian, R.; Meng, S.; Zheng, S.; Sun, X.; Wei, M. Thermo-hydraulic performance evaluation of lattice structures with triply periodic minimal surfaces for latent heat storage devices. *J. Energy Storage* **2024**, *102*, 114234. [CrossRef]
157. Tian, Y.; Liu, X.; Luo, Q.; Yao, H.; Wang, J.; Dang, C.; Lv, S.; Xu, Q.; Li, J.; Zhang, L.; et al. Sea urchin skeleton-inspired triply periodic foams for fast latent heat storage. *Int. J. Heat Mass Transf.* **2023**, *206*, 123944. [CrossRef]
158. Turner, D.; Howie, R.; Bland, P. The development of a next-generation latticed resistojet thruster for CubeSats. *Aerospace* **2024**, *11*, 714. [CrossRef]
159. Vignoles, G.L.; Rochais, D.; Chupin, S. Computation of the conducto-radiative effective heat conductivity of porous media defined by Triply Periodic Minimal Surfaces. *Int. J. Therm. Sci.* **2021**, *159*, 106598. [CrossRef]

160. Wang, F.; Jiang, H.; Chen, Y.; Li, X. Predicting thermal and mechanical performance of stochastic and architected foams. *Int. J. Heat Mass Transf.* **2021**, *171*, 121139. [CrossRef]
161. Wang, J.; Chen, K.; Zeng, M.; Ma, T.; Wang, Q.; Cheng, Z. Assessment of flow and heat transfer of triply periodic minimal surface based heat exchangers. *Energy* **2023**, *282*, 128806. [CrossRef]
162. Wang, J.; Chen, K.; Zeng, M.; Ma, T.; Wang, Q.; Cheng, Z. Investigation on flow and heat transfer in various channels based on triply periodic minimal surfaces (TPMS). *Energy Convers. Manag.* **2023**, *283*, 116955. [CrossRef]
163. Wang, J.; Pu, W.; Zhao, H.; Qiao, L.; Song, N.; Yue, C. Experimental and numerical investigations on the intermittent heat transfer performance of phase change material (PCM)-based heat sink with triply periodic minimal surfaces (TPMS). *Appl. Therm. Eng.* **2024**, *254*, 123864. [CrossRef]
164. Wang, J.; Pu, W.; Zhao, H.; Qiao, L.; Song, N.; Yue, C. Investigations on the heat transfer performance of phase change material (PCM)-based heat sink with triply periodic minimal surfaces (TPMS). *Int. J. Heat Mass Transf.* **2024**, *234*, 126078. [CrossRef]
165. Wang, J.; Qian, C.; Yu, B.; Zhang, F.; Ma, R.; Shi, J.; Chen, J. Design and optimization of additive manufactured Fischer-Koch-structured heat exchanger for enhanced heat transfer efficiency. *Int. Commun. Heat Mass Transf.* **2024**, *159*, 108078. [CrossRef]
166. Wang, J.; Sun, K.; Zeng, M.; Wang, Q.; Cheng, Z. Investigation on uneven flow distribution in triply periodic minimal surface heat exchangers. *Energy Convers. Manag.* **2024**, *314*, 118713. [CrossRef]
167. Wang, S.; Jiang, Y.; Hu, J.; Fan, X.; Luo, Z.; Liu, Y.; Liu, L. Efficient Representation and Optimization of TPMS-Based Porous Structures for 3D Heat Dissipation. *Comput.-Aided Des.* **2022**, *142*, 103123. [CrossRef]
168. Wang, J.; Qian, C.; Qiu, X.; Yu, B.; Yan, L.; Shi, J.; Chen, J. Numerical and experimental investigation of additive manufactured heat exchanger using triply periodic minimal surfaces (TPMS). *Therm. Sci. Eng. Prog.* **2024**, *55*, 103007. [CrossRef]
169. Xia, Q.; Zhu, J.; Yu, Q.; Kim, J.; Li, Y. Triply periodic minimal surfaces based topology optimization for the hydrodynamic and convective heat transfer. *Commun. Nonlinear Sci. Numer. Simul.* **2024**, *131*, 107819. [CrossRef]
170. Xiong, S.; Wang, Z.; Bao, R.; Yang, H.; Zhang, B.; Du, X. Performance study and optimization of hybrid battery thermal management system based on triply periodic minimal surface coupled phase change material. *J. Energy Storage* **2024**, *100*, 113529. [CrossRef]
171. Xu, H.; Yu, W.; Zhang, Y.; Ma, S.; Wu, Z.; Liu, X. Flow and heat transfer performance of bionic heat transfer structures with hybrid triply periodic minimal surfaces. *Appl. Energy* **2023**, *351*, 121847. [CrossRef]
172. Xu, D.; Lin, M. Design controllable TPMS structures for solar thermal applications: A pore-scale vs. volume-averaged modeling approach. *Int. J. Heat Mass Transf.* **2023**, *201*, 123625. [CrossRef]
173. Xu, S.; He, M.; Xu, Z.; Yang, K. Thermology-mechanical integrated SiC panel with triply periodic minimal surface architectures for thermal protection. *Addit. Manuf.* **2024**, *80*, 103981. [CrossRef]
174. Yan, K.; Deng, H.; Xiao, Y.; Wang, J.; Luo, Y.; Yan, J. Influence of polishing process on surface morphology and thermo-hydraulic performance of additively manufactured Gyroid-structured heat exchanger. *Appl. Therm. Eng.* **2024**, *253*, 123828. [CrossRef]
175. Yan, G.; Liu, Y.; Zhang, Z.; Sun, M.; Li, S.; Zhang, X.; Jiang, L.; Xing, S.; Mao, Y. Thermal-hydraulic performance of modified Schwartz-Diamond solid-networks triply periodic minimal surface structures. *Appl. Therm. Eng.* **2024**, *249*, 123384. [CrossRef]
176. Yan, G.; Sun, M.; Liang, Y.; Li, S.; Zhang, Z.; Zhang, X.; Song, Y.; Liu, Y.; Zhao, J. Simulation and experimental study on flow and heat transfer performance of sheet-network and solid-network disturbance structures based on triply periodic minimal surface. *Int. J. Heat Mass Transf.* **2024**, *219*, 124905. [CrossRef]
177. Yan, G.; Sun, M.; Zhang, Z.; Liang, Y.; Jiang, N.; Pang, X.; Song, Y.; Liu, Y.; Zhao, J. Experimental study on flow and heat transfer performance of triply periodic minimal surface structures and their hybrid form as disturbance structure. *Int. Commun. Heat Mass Transf.* **2023**, *147*, 106942. [CrossRef]
178. Yan, K.; Deng, H.; Xiao, Y.; Wang, J.; Luo, Y. Thermo-hydraulic performance evaluation through experiment and simulation of additive manufactured Gyroid-structured heat exchanger. *Appl. Therm. Eng.* **2024**, *241*, 122402. [CrossRef]
179. Yan, K.; Wang, J.; Li, L.; Deng, H. Numerical investigation into thermo-hydraulic characteristics and mixing performance of triply periodic minimal surface-structured heat exchangers. *Appl. Therm. Eng.* **2023**, *230*, 120748. [CrossRef]
180. Yang, Z.; Zhang, T.; Li, W.; Zhou, Y.; Li, X.; Liu, F. Experimental and numerical assessments of thermal transport in phase change material embedding additively manufactured triply periodic minimal surfaces: A comparative evaluation. *Appl. Therm. Eng.* **2024**, *245*, 122850. [CrossRef]
181. Yang, C.; Wu, W.; Fu, Z.; Zheng, H. Preparation and thermal insulation properties of TPMS 3Y-TZP ceramics using DLP 3D printing technology. *J. Mater. Sci.* **2023**, *58*, 11992–12007. [CrossRef]
182. Ye, H.; Tian, F.; He, W.; Wang, S. Mechanical and thermal property analysis and optimization design of hybrid lattice structure based on triply periodic minimal surfaces. *Thin-Walled Struct.* **2024**, *203*, 112203. [CrossRef]
183. Yeranee, K.; Rao, Y. Turbulent Flow and Heat Transfer Enhancement for Turbine Blade Trailing Edge Cooling with Gyroid-Type Triply Periodic Minimal Surfaces. *J. Eng. Gas Turbines Power* **2023**, *145*, 071008. [CrossRef]

184. Yeranee, K.; Rao, Y.; Xu, C.; Xie, J.; Zhang, Y. Conjugate heat transfer and fluid flow analysis on printable double-wall effusion cooling with internal topology-optimized TPMS structures. *Therm. Sci. Eng. Prog.* **2024**, *55*, 102939. [CrossRef]
185. Yeranee, K.; Rao, Y.; Xu, C.; Zhang, Y.; Su, X. Turbulent Flow Heat Transfer and Thermal Stress Improvement of Gas Turbine Blade Trailing Edge Cooling with Diamond-Type TPMS Structure. *Aerospace* **2023**, *11*, 37. [CrossRef]
186. Yeranee, K.; Rao, Y.; Zuo, Q.; Xie, J. Thermal performance enhancement for gas turbine blade trailing edge cooling with topology-optimized printable diamond TPMS lattice. *Int. J. Heat Fluid Flow* **2024**, *110*, 109649. [CrossRef]
187. Yeranee, K.; Xu, C.; Rao, Y.; Chen, J.; Zhang, Y. Rotating Flow and Heat Transfer Characteristics of a Novel Cooling Channel for Gas Turbine Blade Trailing Edge with Diamond-Type TPMS Structures. *ASME J. Heat Mass Transf.* **2024**, *146*, 051002. [CrossRef]
188. Yeranee, K.; Rao, Y. Heat Transfer and Pressure Loss of Turbulent Flow in a Wedge-Shaped Cooling Channel with Different Types of Triply Periodic Minimal Surfaces. *ASME J. Heat Mass Transf.* **2023**, *145*, 093901. [CrossRef]
189. Yetik, O.; Engün, S.; Kok, B.; Karakoc, T.H. Thermal management system of batteries using AlN reinforced TPMS-PCM composite material. *Energy* **2024**, *313*, 134137. [CrossRef]
190. You, H.; Lee, S.; Baek, C.; Han, C.; Kim, Y. Enhancement of heat transfer in cooling channels for electronic devices using multi-directional graded triply periodic minimal surfaces (TPMS). *Int. Commun. Heat Mass Transf.* **2024**, *159*, 108278. [CrossRef]
191. Zhang, T.; Liu, F.; Deng, X.; Zhao, M.; Zhou, H.; Zhang, D.Z. Experimental study on the thermal storage performance of phase change materials embedded with additively manufactured triply periodic minimal surface architected lattices. *Int. J. Heat Mass Transf.* **2022**, *199*, 123452. [CrossRef]
192. Zhang, T.; Liu, F.; Zhang, K.; Zhao, M.; Zhou, H.; Zhang, D.Z. Numerical study on the anisotropy in thermo-fluid behavior of triply periodic minimal surfaces (TPMS). *Int. J. Heat Mass Transf.* **2023**, *215*, 124541. [CrossRef]
193. Zhang, T.; Zhang, K.; Liu, F.; Zhao, M.; Zhang, D.Z. Analysis of thermal storage behavior of composite phase change materials embedded with gradient-designed TPMS thermal conductivity enhancers: A numerical and experimental study. *Appl. Energy* **2024**, *358*, 122630. [CrossRef]
194. Zhang, X.; Li, H.; Dong, H.; Zhang, Y.; Sun, M.; Song, Y. Thermal performance of phase change materials embedded in functional gradient triply periodic minimal surface structures. *J. Energy Storage* **2024**, *100*, 113636. [CrossRef]
195. Zhang, L.; Li, Y.; Hu, R.; Yin, J.; Sun, Q.; Li, X.; Gao, L.; Wang, H.; Xiong, W.; Hao, L. Freeform thermal-mechanical Bi-functional Cu-plated diamond/Cu metamaterials manufactured by selective laser melting. *J. Alloys Compd.* **2023**, *968*, 172010. [CrossRef]
196. Zhao, Y.; Li, M.; Chen, J.; Zeng, Y. Performance improvement of additively manufactured complex configuration of polyamide 12. *Addit. Manuf. Front.* **2024**, *3*, 200165. [CrossRef]
197. Zhou, J.; Chen, H.; Gong, B.; Wang, X.; Cai, J.; Cai, C.; Shi, Y. Comparison between tritium breeders with pebble bed and Gyroid block configurations using numerical investigation: Flow behavior and heat transfer performance. *Case Stud. Therm. Eng.* **2024**, *60*, 104778. [CrossRef]
198. Zhou, Z.; Chen, L.; Wang, W.; Xing, B.; Tian, J.; Zhao, Z. Effective thermal conductivity and heat transfer characteristics of a series of ceramic triply periodic minimal surface lattice structure. *Adv. Eng. Mater.* **2023**, *25*, 2300359. [CrossRef]
199. Zhou, Z.; Lv, Y.; He, F.; Liu, T.; Wang, J. Pore-scale investigation of transpiration cooling based on triply periodic minimal surface. *Int. J. Therm. Sci.* **2024**, *201*, 109019. [CrossRef]
200. Natural Earth. Natural Earth Admin 0—Countries (1:110m), GeoJSON. Public Domain Dataset. 2024. Available online: https://www.naturalearthdata.com (accessed on 16 October 2025).
201. Al-Ketan, O.; Abu Al-Rub, R.K. MSLattice: A free software for generating uniform and graded lattices based on triply periodic minimal surfaces. *Mater. Des. Process. Commun.* **2021**, *3*, e205. [CrossRef]
202. nTopology Inc. nTopology. 2024. Available online: https://ntopology.com (accessed on 16 October 2024).
203. The MathWorks Inc. MATLAB. 2024. Available online: https://www.mathworks.com (accessed on 16 October 2025).
204. Belhadj, H. MathMod. 2024. Available online: https://www.mathmod.org (accessed on 16 October 2025).
205. Dassault Systèmes. SOLIDWORKS. 2024. Available online: https://www.solidworks.com (accessed on 16 October 2025).
206. Siemens Digital Industries Software. Siemens NX. 2024. Available online: https://www.plm.automation.siemens.com (accessed on 16 October 2025).
207. ANSYS Inc. ANSYS Fluent. 2024. Available online: https://www.ansys.com (accessed on 16 October 2025).
208. Math2Market GmbH. GeoDict. 2024. Available online: https://www.geodict.com (accessed on 16 October 2025).
209. Wolfram Research. Mathematica. 2024. Available online: https://www.wolfram.com/mathematica (accessed on 16 October 2025).
210. Robert McNeel & Associates. Rhinoceros 3D. 2024. Available online: https://www.rhino3d.com (accessed on 16 October 2025).
211. Ali Soltani. MaSMaker. 2024. Available online: https://github.com/alisoltani/MaSMaker (accessed on 16 October 2025).
212. hiilda. TPMS Lattice Generator (LattGen). GitHub Repository. 2025. Available online: https://github.com/hiilda/TPMS-Lattice-Generator-LattGen- (accessed on 16 October 2025).

213. Narasimharaju, S.R.; Zeng, W.; See, T.L.; Zhu, Z.; Scott, P.; Jiang, X.; Lou, S. A comprehensive review on laser powder bed fusion of steels: Processing, microstructure, defects and control methods, mechanical properties, current challenges and future trends. *J. Manuf. Processes* **2022**, *75*, 375–414. [CrossRef]
214. Sefene, E.M. State-of-the-art of selective laser melting process: A comprehensive review. *J. Manuf. Syst.* **2022**, *63*, 250–274. [CrossRef]
215. Song, Y.; Ghafari, Y.; Asefnejad, A.; Toghraie, D. An overview of selective laser sintering 3D printing technology for biomedical and sports device applications: Processes, materials, and applications. *Opt. Laser Technol.* **2024**, *171*, 110459. [CrossRef]
216. Pfeiffer, S.; Florio, K.; Puccio, D.; Grasso, M.; Colosimo, B.M.; Aneziris, C.G.; Wegener, K.; Graule, T. Direct laser additive manufacturing of high performance oxide ceramics: A state-of-the-art review. *J. Eur. Ceram. Soc.* **2021**, *41*, 6087–6114. [CrossRef]
217. Kushwaha, A.K.; Rahman, M.H.; Hart, D.; Hughes, B.; Saldana, D.A.; Zollars, C.; Rajak, D.K.; Menezes, P.L. Fundamentals of stereolithography: Techniques, properties, and applications. In *Tribology of Additively Manufactured Materials*; Elsevier: Amsterdam, The Netherlands, 2022; pp. 87–106. [CrossRef]
218. Penumakala, P.K.; Santo, J.; Thomas, A. A critical review on the fused deposition modeling of thermoplastic polymer composites. *Compos. Part B Eng.* **2020**, *201*, 108336. [CrossRef]
219. Chaudhary, R.; Fabbri, P.; Leoni, E.; Mazzanti, F.; Akbari, R.; Antonini, C. Additive manufacturing by digital light processing: A review. *Prog. Addit. Manuf.* **2023**, *8*, 331–351. [CrossRef]
220. Siemens Digital Industries Software. STAR-CCM+. 2024. Available online: https://www.plm.automation.siemens.com/products/star-ccm (accessed on 16 October 2025).
221. COMSOL Inc. COMSOL Multiphysics. 2024. Available online: https://www.comsol.com (accessed on 16 October 2025).
222. The OpenFOAM Foundation. OpenFOAM. 2024. Available online: https://www.openfoam.org (accessed on 16 October 2025).
223. Simerics Inc. Simerics-MP. 2024. Available online: https://www.simerics.com/products/simerics-mp (accessed on 16 October 2025).
224. Palabos Project. Palabos. 2024. Available online: https://palabos.unige.ch (accessed on 16 October 2025).
225. Dierkes, U.; Hildebrandt, S.; Sauvigny, F. Minimal Surfaces. In *Grundlehren der mathematischen Wissenschaften*; Springer: Berlin/Heidelberg, Germany, 2010; Volume 339.
226. Shaheed, R.; Mohammadian, A.; Kheirkhah Gildeh, H. A comparison of standard k–ε and realizable k–ε turbulence models in curved and confluent channels. *Environ. Fluid Mech.* **2019**, *19*, 543–568. [CrossRef]
227. Difonzo, R.; Gajetti, E.; Savoldi, L.; Fathi, N. Assessment of different RANS turbulence models in mini-channels for the cooling of MW-class gyrotron resonators. *Int. J. Heat Mass Transf.* **2022**, *193*, 122922. [CrossRef]
228. Argyropoulos, C.; Markatos, N. Recent advances on the numerical modeling of turbulent flows. *Appl. Math. Model.* **2015**, *39*, 693–732. [CrossRef]
229. Menter, F.; Kuntz, M.; Langtry, R. Ten years of industrial experience with the SST turbulence model. *Heat Mass Transf.* **2003**, *4*, 625–632.
230. Gajetti, E.; Boccardo, G.; Savoldi, L.; Marocco, L. Hydrodynamic characterization of Gyroid, Diamond and Split-P Triply Periodic Minimal Surfaces as porous medium. *Int. J. Heat Mass Transf.* **2025**, *252*, 127439. [CrossRef]
231. Gee, D.; Webb, R. Forced convection heat transfer in helically rib-roughened tubes. *Int. J. Heat Mass Transf.* **1980**, *23*, 1127–1136. [CrossRef]